Defense Threat Reduction Agency
8725 John J. Kingman Road, MS
6201 Fort Belvoir, VA 22060-6201

DTRA-TR-16-19

TECHNICAL REPORT

Relationships between Liquid Atomization and Solid Fragmentation

March 2016

DTRA1-11-D-0004

Culbert B. Laney

Prepared by:
Engility Corporation
8211 Terminal Road
Lorton, VA 22079

DESTRUCTION NOTICE:

Destroy this report when it is no longer needed.
Do not return to sender.

PLEASE NOTIFY THE DEFENSE THREAT REDUCTION AGENCY, ATTN: DTRIAC/ J9STT, 8725 JOHN J. KINGMAN ROAD, MS-6201, FT BELVOIR, VA 22060-6201, IF YOUR ADDRESS IS INCORRECT, IF YOU WISH IT DELETED FROM THE DISTRIBUTION LIST, OR IF THE ADDRESSEE IS NO LONGER EMPLOYED BY YOUR ORGANIZATION.

REPORT DOCUMENTATION PAGE

Form Approved
OMB No. 0704-0188

1. REPORT DATE *(DD-MM-YYYY)*
00-03-2016

2. REPORT TYPE
Technical

3. DATES COVERED *(From - To)*
N/A

4. TITLE AND SUBTITLE
Relationships between Liquid Atomization and Solid Fragmentation

5a. CONTRACT NUMBER
HDTRA1-11-D-0004

5b. GRANT NUMBER

5c. PROGRAM ELEMENT NUMBER

6. AUTHOR(S)
Culbert B. Laney

5d. PROJECT NUMBER

5e. TASK NUMBER

5f. WORK UNIT NUMBER

7. PERFORMING ORGANIZATION NAME(S) AND ADDRESS(ES)
Engility Corporation
8211 Terminal Road
Lorton, VA 22079

8. PERFORMING ORGANIZATION REPORT NUMBER

9. SPONSORING / MONITORING AGENCY NAME(S) AND ADDRESS(ES)
Defense Threat Reduction Agency
8725 John J. Kingman Road, STOP 6201
Fort Belvoir, VA 22060-6201

10. SPONSOR/MONITOR'S ACRONYM(S)
DTRA

11. SPONSOR/MONITOR'S REPORT NUMBER(S)
DTRA-TR-16-19

12. DISTRIBUTION / AVAILABILITY STATEMENT
Distribution Statement A. Approved for public release; distribution is unlimited.

13. SUPPLEMENTARY NOTES

14. ABSTRACT
This paper surveys fragment size distributions found in the research literature, including specific examples of Weibull, Gamma, and root normal size distributions. This paper finds that, in many instances, the solid and liquid fragmentation communities have independently discovered the same or similar fragment size distributions. In addition, this paper shows that the solid and liquid fragmentation communities have independently discovered nearly the same expressions for average fragment sizes. These observations are surprising, given the fundamental phenomenological differences between liquid and solid fragmentation.

15. SUBJECT TERMS
ragment size distribution, Weibull size distribution, Gamma size distribution, Mott-Linfoot size distribution

16. SECURITY CLASSIFICATION OF:			17. LIMITATION OF ABSTRACT	18. NUMBER OF PAGES	19a. NAME OF RESPONSIBLE PERSON
					Capt. Paul Clement
a. REPORT	**b. ABSTRACT**	**c. THIS PAGE**	UU	59	**19b. TELEPHONE NUMBER** *(include area code)*
Unclassified	Unclassified	Unclassified			703-767-4035

Standard Form 298 (Rev. 8-98)
Prescribed by ANSI Std. Z39.18

UNIT CONVERSION TABLE

U.S. customary units to and from international units of measurement*

U.S. Customary Units	Multiply by → / ← Divide by†		International Units
Length/Area/Volume			
inch (in)	2.54	$\times 10^{-2}$	meter (m)
foot (ft)	3.048	$\times 10^{-1}$	meter (m)
yard (yd)	9.144	$\times 10^{-1}$	meter (m)
mile (mi, international)	1.609 344	$\times 10^{3}$	meter (m)
mile (nmi, nautical, U.S.)	1.852	$\times 10^{3}$	meter (m)
barn (b)	1	$\times 10^{-28}$	square meter (m^2)
gallon (gal, U.S. liquid)	3.785 412	$\times 10^{-3}$	cubic meter (m^3)
cubic foot (ft^3)	2.831 685	$\times 10^{-2}$	cubic meter (m^3)
Mass/Density			
pound (lb)	4.535 924	$\times 10^{-1}$	kilogram (kg)
unified atomic mass unit (amu)	1.660 539	$\times 10^{-27}$	kilogram (kg)
pound-mass per cubic foot (lb ft^{-3})	1.601 846	$\times 10^{1}$	kilogram per cubic meter (kg m^{-3})
pound-force (lbf avoirdupois)	4.448 222		newton (N)
Energy/Work/Power			
electron volt (eV)	1.602 177	$\times 10^{-19}$	joule (J)
erg	1	$\times 10^{-7}$	joule (J)
kiloton (kt) (TNT equivalent)	4.184	$\times 10^{12}$	joule (J)
British thermal unit (Btu) (thermochemical)	1.054 350	$\times 10^{3}$	joule (J)
foot-pound-force (ft lbf)	1.355 818		joule (J)
calorie (cal) (thermochemical)	4.184		joule (J)
Pressure			
atmosphere (atm)	1.013 250	$\times 10^{5}$	pascal (Pa)
pound force per square inch (psi)	6.984 757	$\times 10^{3}$	pascal (Pa)
Temperature			
degree Fahrenheit (°F)	[T(°F) − 32]/1.8		degree Celsius (°C)
degree Fahrenheit (°F)	[T(°F) + 459.67]/1.8		kelvin (K)
Radiation			
curie (Ci) [activity of radionuclides]	3.7	$\times 10^{10}$	per second (s^{-1}) [becquerel (Bq)]
roentgen (R) [air exposure]	2.579 760	$\times 10^{-4}$	coulomb per kilogram (C kg^{-1})
rad [absorbed dose]	1	$\times 10^{-2}$	joule per kilogram (J kg^{-1}) [gray (Gy)]
rem [equivalent and effective dose]	1	$\times 10^{-2}$	joule per kilogram (J kg^{-1}) [sievert (Sv)]

*Specific details regarding the implementation of SI units may be viewed at http://www.bipm.org/en/si/.
†Multiply the U.S. customary unit by the factor to get the international unit. Divide the international unit by the factor to get the U.S. customary unit.

Table of Contents

Table of Figures

Table of Tables

On the Relationships Between Liquid and Solid Fragmentation

Culbert B. Laney[1]
Engility Corp., 8211 Terminal Rd, Lorton, VA 22079 U.S.A.

Abstract. *This paper surveys fragment size distributions found in the research literature, including specific examples of Weibull, Gamma, and root normal size distributions. This paper finds that, in many instances, the solid and liquid fragmentation communities have independently discovered the same or similar fragment size distributions. In addition, this paper shows that the solid and liquid fragmentation communities have independently discovered nearly the same expressions for average fragment sizes. These observations are surprising, given the fundamental phenomenological differences between liquid and solid fragmentation.*

Keywords: fragment size distribution, Weibull size distribution, Gamma size distribution, Mott-Linfoot size distribution, Marshall-Palmer size distribution, Simmons size distribution

1. Introduction

At first glance, it seems that solid and liquid fragmentation have little in common. In typical cases, solids are believed to fragment via multiple propagating cracks originating at strain-induced or pre-existing microstructural flaws. For example, for impact fragmentation of solids, Wittel et. al. (2008) say: "The average size of … fragments … is determined by the relationship between the rate at which cracks nucleate and the velocity of the stress release wave. The higher the strain rate, the higher the crack nucleation rate and the more … cracks are formed."

By contrast, in typical cases, liquids are believed to fragment due to flows resulting in thin surface protrusions such as sheets, ligaments, and so forth. As these surface protrusions stretch, hydrodynamic instabilities grow until the troughs penetrate and pinch off fragments. For example, for jet atomization, Marmottant & Villermaux (2004b) say: "Liquid destabilization proceeds from a two-stage mechanism: a shear instability first forms waves on the liquid. The transient acceleration experienced by the liquid suggests that a Rayleigh–Taylor type of instability is triggered at the wave crests, producing liquid ligaments which further stretch in the air stream and break into droplets."

In typical cases, liquids experience two-stage fragmentation due to aerodynamic forces, i.e., parent droplets created in the primary stage produce smaller children droplets in the secondary stage. The basic phenomenology of the second stage is much the same as that of the first stage. For example, Hsiang & Faeth (1992) observed: "[children] drops or ligaments are stripped from boundary layers … that form near the liquid surface … on the windward side of the [parent] droplet." In some scenarios, solids can also experience multi-stage fragmentation e.g., during grinding or milling. However, this is not as common for solids as it is for liquids.

In addition, in typical cases, liquid fragments experience coagulation – the inverse of fragmentation – due to random collisions between fragments, e.g., Villermaux et. al. (2004). Solid fragments, including small asteroids and dust, may experience something similar due to

[1] E-mail address: Bert.Laney@engilitycorp.com

electrostatic or van der Waals forces. However, this is not as common for solids as it is for liquids.

Despite the apparent lack of similarity between liquid and solid fragmentation, there is a long history of techniques developed for solid fragmentation being used for liquid fragmentation and, to a lesser extent, vice versa. For example, while originally developed for solid fragmentation, Liu (2000) notes that Rosin-Rammler size distributions are "perhaps the most widely used" size distributions for liquid fragmentation; see also Ashgriz (2011). Well-known subsets of Rosin-Rammler size distributions include Weibull (1939a, b) and Griffith (1943). For example, Mott & Linfoot (1943) and Grady & Kipp (1985) use Weibull distributions for solids while Marshall & Palmer (1948) and Li & Tankin (1987) use them for liquids. For another example, Grady & Kipp (1987) use Griffith distribution for solids while Tishkoff & Law (1977) use them for liquids.

More generally, this paper shows that liquid and solid fragmentation often produce similar results, both in terms of average fragment sizes and in terms of the overall fragment size distributions. Because liquid fragmentation tends to produce semi-spherical droplets, liquid fragmentation is usually described by fragment diameters. Because solid fragmentation tends to produce irregular shapes, solid fragmentation is usually described by fragment masses. These and other superficial differences often mask similarities between liquid and solid fragmentation. Building on Laney (2015a, b), this treatment includes techniques for transforming between mass and diameter, and between mass fraction and number fraction.

2. Basic Definitions

Let *D* be the fragment diameter and let *M* be the fragment mass. Four common ways of expressing fragment size distributions are as follows:

> $F(D)$ [$F(M)$] is the number fraction of fragments with diameters [masses] greater than or equal to *D* [*M*]
>
> $F_M(D)$ [$F_M(M)$] is the mass fraction of fragments with diameters [masses] greater than or equal to *D* [*M*].

In standard probability theory, $F(x)$ is called a *complementary cumulative distribution function* (*CCDF*). Notice that $F(x)$ is monotone decreasing such that $F(0)=1$ and $F(\infty)=0$. Alternatively, four common ways of expressing fragment size distributions are as follows

> $f_M(D)$ [$f_M(M)$] is the mass fraction of fragments with diameters [masses] in a range *dD* centered on *D* divided by *dD* [*dM* centered on *M* divided by *dM*]
>
> $f(D)$ [$f(M)$] is the number fraction of fragments with diameters [masses] in a range *dD* centered on *D* divided by *dD* [*dM* centered on *M* divided by *dM*]

In standard probability theory, $f(x)$ is called a *probability density function* (*PDF*). The following eight equations may be used to transform between the above eight expressions:

$$M = c\rho D^m \tag{1}$$

$$F_M(M) = F_M(D) \tag{2}$$

$$F(M) = F(D) \tag{3}$$

$$f_M(D) = \text{const.}\, D^m f(D)\,;\;\; f_M(M) = \text{const.}\, Mf(M) \tag{4}$$

$$F_M(D) = -\int_D^\infty f_M(x)dx\,;\;\; f_M(D) = -\frac{dF_M}{dD} \tag{5}$$

$$F_M(M) = -\int_M^\infty f_M(x)dx\,;\;\; f_M(M) = -\frac{dF_M}{dM} \tag{6}$$

$$F(D) = -\int_D^\infty f(x)dx\,;\;\; f(D) = -\frac{dF}{dD} \tag{7}$$

$$F(M) = -\int_M^\infty f(x)dx\,;\;\; f(M) = -\frac{dF}{dM} \tag{8}$$

where m is the fragment dimension, ρ is the fragment density, and c is a constant. Notice that liquids tend to produce spherical fragments with $m = 3$ while solids may produce irregular fragments with any $1 \le m \le 3$.

Table 1 defines eight possible average fragment sizes in terms of $f(x)$ and $f_M(x)$.

Table 1. Eight possible average fragment sizes. Asterisks (*) indicate non-standard terminology.

Notation	Definition	Name	Notation	Definition	Name
D_{avg}	$\int_0^\infty Df(D)dD$	Count Mean Diameter (CMD)	M_{avg}	$\int_0^\infty Mf(M)dM$	Count Mean Mass (CMM) (*)
$D_{M\,avg}$	$\int_0^\infty D\, f_M(D)dD$	Mass Mean Diameter (MMD)	$M_{M\,avg}$	$\int_0^\infty M\, f_M(M)dM$	Mass Mean Mass (MMM) (*)
D'_{avg}	$\dfrac{1}{\int_0^\infty \frac{f(D)}{D}dD}$	Sauter Count Mean Diameter (SCMD) (*)	M'_{avg}	$\dfrac{1}{\int_0^\infty \frac{f(M)}{M}dM}$	Sauter Count Mean Mass (SCMM) (*)
$D'_{M\,avg}$	$\dfrac{1}{\int_0^\infty \frac{f_M(D)}{D}dD}$	Sauter Mass Mean Diameter (SMMD)	$M'_{M\,avg}$	$\dfrac{1}{\int_0^\infty \frac{f_M(M)}{M}dM}$	Sauter Mass Mean Mass (SMMM) (*)

Consider the following ratio of averages:

$$R_M = \frac{D_{M\ avg}}{D'_{M\ avg}} \tag{10}$$

This is a measure of fragment size spread. While traditionally used for liquid fragmentation, it is equally valid for solid fragmentation. As an empirical observation, different fragment size distributions are often almost the same when R_M is almost the same.

Similarly, consider the following ratio of averages:

$$S = \frac{M_{avg}}{\rho c D_{avg}^m} \tag{11}$$

3. Fragment Size Distributions

This section summarizes some of the key results from Laney (2015a, b).

3.1 Weibull Size Distributions

Table 2 shows eight different forms of Type I Weibull size distributions. These are also known as Rosin-Rammmler-Sperling-Bennett (RRSB) size distributions; see Rosin et. al (1933) and Bennett (1936). Table 3 shows eight different forms for Type II Weibull size distributions; see Weibull (1939a, b). In either case, the two free parameters are *n* and an average fragment size. Table 4 gives expressions for the remaining parameters, which depend only on the free parameter *n* and the spatial dimension *m*, and not on the average fragment size. As described by Laney (2015b), Type I and II Weibull size distributions are subsets of Rosin-Rammler (1927) size distributions.

Laney (2015b) defines Type I, II, III, and IV size distributions as follows:

Type I	Type II	Type III	Type IV
$f_M(D)$	$f(D)$	$f_M(M)$	$f(M)$

where all four types have the same general form. Equivalently:

Type I	Type II	Type III	Type IV
$F_M(D)$	$F(D)$	$F_M(M)$	$F(M)$

where all four types have the same general form.

With simple parameter adjustments, Type III Weibull size distributions turn out to be essentially the same as Type I Weibull size distributions, and Type IV Weibull size distributions turn out to be essentially the same as Type II Weibull size distributions.

Table 2a. Type I Weibull size distributions expressed in terms of *F* and *f*.

$F(D) = \dfrac{\Gamma\left[1 - \dfrac{m}{n}, b\left(\dfrac{D}{D_{avg}}\right)^n\right]}{\Gamma\left(1 - \dfrac{m}{n}\right)}$	$F(M) = \dfrac{\Gamma\left[1 - \dfrac{m}{n}, c\left(\dfrac{M}{M_{avg}}\right)^{\frac{n}{m}}\right]}{\Gamma\left(1 - \dfrac{m}{n}\right)}$
$f(D) = \dfrac{1}{AD_{avg}}\left(\dfrac{D}{D_{avg}}\right)^{n-m-1} \exp\left[-b\left(\dfrac{D}{D_{avg}}\right)^n\right]$	$f(M) = \dfrac{S}{mAM_{avg}}\left(\dfrac{SM}{M_{avg}}\right)^{\frac{n}{m}-2} \exp\left[-c\left(\dfrac{M}{M_{avg}}\right)^{\frac{n}{m}}\right]$

Table 2b. Type I Weibull size distributions expressed in terms of F_M and f_M.

$F_M(D) = \exp[-b(D/D_{avg})^n]$	$F_M(M) = \exp[-c(M/M_{avg})^{n/m}]$
$f_M(D) = \dfrac{1}{BD_{avg}}\left(\dfrac{D}{D_{avg}}\right)^{n-1} \exp\left[-b\left(\dfrac{D}{D_{avg}}\right)^n\right]$	$f_M(M) = \dfrac{S}{mBM_{avg}}\left(\dfrac{SM}{M_{avg}}\right)^{n/m-1} \exp\left[-c\left(\dfrac{M}{M_{avg}}\right)^{\frac{n}{m}}\right]$

Table 3a. Type II Weibull size distributions expressed in terms of *F* and *f*.

$F(D) = \exp[-b(D/D_{avg})^n]$	$F(M) = \exp[-c(M/M_{avg})^{n/m}]$
$f(D) = \dfrac{1}{AD_{avg}}\left(\dfrac{D}{D_{avg}}\right)^{n-1} \exp\left[-b\left(\dfrac{D}{D_{avg}}\right)^n\right]$	$f(M) = \dfrac{S}{mAM_{avg}}\left(\dfrac{SM}{M_{avg}}\right)^{n/m-1} \exp\left[-c\left(\dfrac{M}{M_{avg}}\right)^{n/m}\right]$

Table 3b. Type II Weibull size distributions expressed in terms of F_M and f_M.

$F_M(D) = \dfrac{\Gamma\left[1 + m/n, b\left(D/D_{avg}\right)^n\right]}{\Gamma(1 + m/n)}$	$F_M(M) = \dfrac{\Gamma\left[1 + m/n, c\left(M/M_{avg}\right)^{n/m}\right]}{\Gamma(1 + m/n)}$
$f_M(D) = \dfrac{1}{BD_{avg}}\left(\dfrac{D}{D_{avg}}\right)^{n+m-1} \exp\left[-b\left(\dfrac{D}{D_{avg}}\right)^n\right]$	$f_M(M) = \dfrac{S}{mBM_{avg}}\left(\dfrac{SM}{M_{avg}}\right)^{n/m} \exp\left[-c\left(\dfrac{M}{M_{avg}}\right)^{n/m}\right]$

Table 4. Parameters for Type I and II Weibull size distributions which ensure the correct D_{avg} and M_{avg}.

	I	II
b	$\dfrac{\Gamma\left(1-\frac{m-1}{n}\right)^{n}}{\Gamma\left(1-\frac{m}{n}\right)^{n}}$	$\Gamma\left(1+\frac{1}{n}\right)^{n}$
c	$\Gamma\left(1-\frac{m}{n}\right)^{-\frac{n}{m}}$	$\Gamma\left(1+\frac{m}{n}\right)^{\frac{n}{m}}$
S	$\dfrac{b^{-\frac{m}{n}}}{\Gamma\left(1-\frac{m}{n}\right)}$	$b^{-\frac{m}{n}}\,\Gamma\left(1+\frac{m}{n}\right)$
A	$\frac{1}{\lvert n\rvert}\,b^{-\left(1-\frac{m}{n}\right)}\,\Gamma\left(1-\frac{m}{n}\right)$	$\frac{1}{\lvert n\rvert b}$
B	$\frac{1}{\lvert n\rvert b}$	$\frac{1}{\lvert n\rvert}\,b^{-\left(1+\frac{m}{n}\right)}\,\Gamma\left(1+\frac{m}{n}\right)$

The research literature usually considers Weibull size distributions to be the same when n/m is the same. For example, by this convention, $n=1, m=1$ and $n=2, m=2$ and $n=3, m=3$ are all the same while $n=1, m=1$ and $n=1, m=2$ and $n=1, m=3$ are all different.

Figure 1 compares Type I and II Weibull size distributions to test data from Rosin & Rammler (1934). The smallest fragments appear to obey a power law or, equivalently, a negative Weibull size distribution while the largest fragments appear to obey a positive Weibull size distribution. Brown & Wohletz (1995) suggest that “the data consist of two populations: fines that experienced a single fragmentation event and remained unaffected in spaces among larger particles that were repeatedly fragmented during milling.” Notice that the Type II Weibull size distribution provides a somewhat better fit to the test data than the Type I Weibull size distribution. This tends to be true in general. Thus this treatment will rely predominantly on Type II Weibull size distributions.

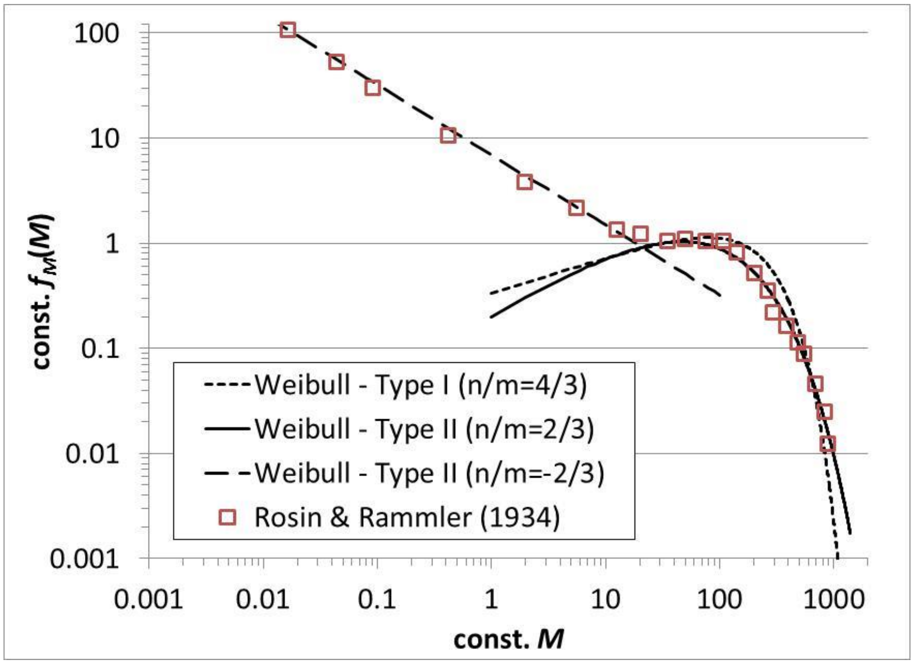

Figure 1. Type I and II Weibull size distributions vs. test data for ball-milling of iron from Rosin & Rammler (1934). A similar figure appeared earlier in Brown & Wohletz (1995).

3.2 Gamma Size Distributions

Table 5 shows eight different forms of Type IIB Gamma size distributions; see, e.g., Villermaux et. al. (2004). Table 6 shows eight different forms for Type IVB Gamma size distributions; see, e.g., Melzak (1953). In either case, the two free parameters are *b* and an average fragment size. Table 7 gives expressions for the remaining parameters, which depend only on the free parameter *b* and the spatial dimension *m*, and not on the average fragment size. As described by Laney (2015b), Type II and IV Weibull size distributions are subsets of Rosin-Rammler (1927) size distributions.

It is also possible to define Type I and III Gamma size distributions. Unlike Weibull size distributions, Type I, II, III and IV Gamma size distributions are all distinct.

For Type IA, IIA, IIIA, and IVA Gamma size distributions, the independent variable is normalized by the mass mean diameter or mass mean mass. Similarly, for Type IB, IIB, IIIB, and IVB Gamma size distributions, the independent variable is normalized by the count mean diameter or count mean mass. For Weibull size distributions, the parameters are the same regardless of normalization; therefore, there is no need to distinguish *A* from *B*. However, for Gamma size distribution, the parameters change along with the normalization; therefore, it is important to distinguish *A* from *B*.

Table 5a. Type IIB Gamma distributions for expressed in terms of *F* and *f*.

$F(D) = \dfrac{\Gamma\left[b, b\dfrac{D}{D_{avg}}\right]}{\Gamma(b)}$	$F(M) = \dfrac{\Gamma\left[b, c\left(\dfrac{M}{M_{avg}}\right)^{1/m}\right]}{\Gamma(b)}$
$f(D) = \dfrac{1}{AD_{avg}}\left(\dfrac{D}{D_{avg}}\right)^{b-1}\exp\left[-b\dfrac{D}{D_{avg}}\right]$	$f(M) = \dfrac{S}{mAM_{avg}}\left(\dfrac{SM}{M_{avg}}\right)^{b/m-1}\exp\left[-c\left(\dfrac{M}{M_{avg}}\right)^{1/m}\right]$

Table 5b. Type IIB Gamma distributions expressed in terms of F_M and f_M.

$F_M(D) = \dfrac{\Gamma\left[b+m, \dfrac{D}{D_{avg}}\right]}{\Gamma(b+m)}$	$F_M(M) = \dfrac{\Gamma\left[b+m, c\left(\dfrac{M}{M_{avg}}\right)^{1/m}\right]}{\Gamma(b+m)}$
$f_M(D) = \dfrac{1}{BD_{avg}}\left(\dfrac{D}{D_{avg}}\right)^{b+m-1}\exp\left[-b\dfrac{D}{D_{avg}}\right]$	$f_M(M) = \dfrac{S}{mBM_{avg}}\left(\dfrac{SM}{M_{avg}}\right)^{b/m}\exp\left[-c\left(\dfrac{M}{M_{avg}}\right)^{1/m}\right]$

Table 6a. Type IVB Gamma distributions for expressed in terms of *F* and *f*.

$F(D) = \dfrac{\Gamma\left[b, c\left(\dfrac{D}{D_{avg}}\right)^{m}\right]}{\Gamma(b)}$	$F(M) = \dfrac{\Gamma\left[b, b\dfrac{M}{M_{avg}}\right]}{\Gamma(b)}$
$f(D) = \dfrac{m}{ASD_{avg}}\left(\dfrac{D}{SD_{avg}}\right)^{mb-1}\exp\left[-c\left(\dfrac{D}{D_{avg}}\right)^{m}\right]$	$f(M) = \dfrac{1}{AM_{avg}}\left(\dfrac{M}{M_{avg}}\right)^{b-1}\exp\left[-b\dfrac{M}{M_{avg}}\right]$

Table 6b. Type IVB Gamma distributions expressed in terms of F_M and f_M.

$F_M(D) = \dfrac{\Gamma\left[b+1, c\left(\dfrac{D}{D_{avg}}\right)^{m}\right]}{\Gamma(b+1)}$	$F_M(M) = \dfrac{\Gamma\left[b+1, b\dfrac{M}{M_{avg}}\right]}{\Gamma(b+1)}$
$f_M(D) = \dfrac{m}{BSD_{avg}}\left(\dfrac{D}{SD_{avg}}\right)^{m(b+1)-1}\exp\left[-c\left(\dfrac{D}{D_{avg}}\right)^{m}\right]$	$f_M(M) = \dfrac{1}{BM_{avg}}\left(\dfrac{M}{M_{avg}}\right)^{b}\exp\left[-b\dfrac{M}{M_{avg}}\right]$

Table 7. Parameters for Type IIB and IVB Gamma size distributions which ensure the correct D_{avg} and M_{avg}.

	IIB	IVB
c	$\dfrac{\Gamma(b+m)^{1/m}}{\Gamma(b)^{1/m}}$	$\dfrac{\Gamma(b+1/m)^{m}}{\Gamma(b)^{m}}$
S	$\dfrac{1}{b^m}\dfrac{\Gamma(b+m)}{\Gamma(b)}$	$\dfrac{b^{1/m}\Gamma(b)}{\Gamma(b+1/m)}$
A	$\dfrac{\Gamma(b)}{b^b}$	$\dfrac{\Gamma(b)}{b^b}$
B	$\dfrac{\Gamma(b+m)}{b^{b+m}}$	$\dfrac{\Gamma(b+1)}{b^{b+1}}$

3.3 Root Normal Size Distributions

Table 8 shows eight different forms of Type IA root normal size distributions; see Tate & Marshall (1953). Table 10 shows eight different forms of Type IIB root normal size distributions; see Laney (2015a). In either case, the two free parameters are σ and an average fragment size. Tables 9 and 11 give expressions for the remaining parameters, which depend only on the free parameter σ and the spatial dimension m, and not on any average fragment size. Most previous treatments let a = 1 and did not attempt to solve the implicit equation for a given in Tables 8 and 10. This means that most previous treatments have errors in the average size.

Table 8a. Type IA root normal distributions expressed in terms of F and f.

$F(D) = -\int_D^{\infty} f(x)dx$	$F(M) = -\int_M^{\infty} f(x)dx$
$f(D) = \dfrac{1}{BD_{M\,avg}}\dfrac{1}{\sqrt{2\pi\sigma^2}}\times \left(\dfrac{D}{D_{M\,avg}}\right)^{-m-1/2}\exp\left[-\dfrac{1}{2\sigma^2}(\sqrt{D/D_{M\,avg}}-a)^2\right]$	$f(M) = \dfrac{S_M}{BmM_{M\,avg}}\dfrac{1}{\sqrt{2\pi\sigma^2}}\times \left(\dfrac{S_M M}{M_{M\,avg}}\right)^{\frac{1}{2m}-2}\exp\left\{-\dfrac{1}{2\sigma^2}\left[\left(\dfrac{S_M M}{M_{M\,avg}}\right)^{\frac{1}{2m}}-a\right]^2\right\}$

Table 8b. Type IA root normal distributions expressed in terms of F_M and f_M

$F_M(D) = \dfrac{1}{A}\mathrm{erfc}\left(\dfrac{\sqrt{D/D_{M\,avg}}-a}{\sqrt{2}\sigma}\right)$	$F_M(M) = \dfrac{1}{A}\mathrm{erfc}\left(\dfrac{(S_M M/M_{M\,avg})^{1/2m}-a}{\sqrt{2}\sigma}\right)$
$f_M(D) = \dfrac{1}{AD_{M\,avg}}\dfrac{1}{\sqrt{2\pi\sigma^2}}\times \dfrac{1}{\sqrt{D/D_{M\,avg}}}\exp\left[-\dfrac{1}{2\sigma^2}(\sqrt{D/D_{M\,avg}}-a)^2\right]$	$f_M(M) = \dfrac{S_M}{AmM_{M\,avg}}\dfrac{1}{\sqrt{2\pi\sigma^2}}\times \left(\dfrac{S_M M}{M_{M\,avg}}\right)^{\frac{1}{2m}-1}\exp\left\{-\dfrac{1}{2\sigma^2}\left[\left(\dfrac{S_M M}{M_{M\,avg}}\right)^{\frac{1}{2m}}-a\right]^2\right\}$

Table 9. Parameters for Type IA root normal size distributions which ensure the correct $D_{M\,avg}$ and $M_{M\,avg}$.

A	$\sigma^2 + a^2 + \frac{2\sigma a}{\sqrt{2\pi}} \frac{\exp(-a^2/2\sigma^2)}{\mathrm{erfc}(-a/\sqrt{2}\sigma)} = 1$ (implicit equation)
A	$\mathrm{erfc}\left(-\frac{a}{\sqrt{2}\sigma}\right)$
B	$\frac{1}{\sqrt{2\pi\sigma^2}} \int_\delta^\infty x^{-m-1/2} \exp\left[-\frac{(\sqrt{x}-a)^2}{2\sigma^2}\right] dx$
S_M	$a^6 + 15a^4\sigma^2 + 45a^2\sigma^4 + 15\sigma^6 + (a^4 + 14a^2\sigma^2 + 33\sigma^4)\frac{2\sigma a}{\sqrt{2\pi}} \exp\left(-\frac{a^2}{2\sigma^2}\right) \Big/ \mathrm{erfc}\left(-\frac{a}{\sqrt{2}\sigma}\right)$

Table 10a. Root normal distributions of Type IIB expressed in terms of F and f.

$F(D) = \frac{1}{A}\mathrm{erfc}\left(\frac{\sqrt{D/D_{avg}} - a}{\sqrt{2}\sigma}\right)$	$F(M) = \frac{1}{A}\mathrm{erfc}\left(\frac{(SM/M_{avg})^{1/2m} - a}{\sqrt{2}\sigma}\right)$
$f(D) = \frac{1}{AD_{avg}} \frac{1}{\sqrt{2\pi\sigma^2}} \times \frac{1}{\sqrt{D/D_{avg}}} \exp\left[-\frac{1}{2\sigma^2}(\sqrt{D/D_{avg}} - a)^2\right]$	$f(M) = \frac{S}{AmM_{avg}} \frac{1}{\sqrt{2\pi\sigma^2}} \times \left(\frac{SM}{M_{avg}}\right)^{\frac{1}{2m}-1} \exp\left\{-\frac{1}{2\sigma^2}\left[\left(\frac{SM}{M_{avg}}\right)^{\frac{1}{2m}} - a\right]^2\right\}$

Table 10b. Root normal distributions of Type IIB expressed in terms of F_M and f_M.

$F_M(D) = -\int_D^\infty f_M(x)dx$	$F_M(M) = -\int_M^\infty f_M(x)dx$
$f_M(D) = \frac{1}{BD_{avg}} \frac{1}{\sqrt{2\pi\sigma^2}} \times \left(\frac{D}{D_{avg}}\right)^{m-1/2} \exp\left[-\frac{1}{2\sigma^2}(\sqrt{D/D_{avg}} - a)^2\right]$	$f_M(M) = \frac{S}{BmM_{avg}} \frac{1}{\sqrt{2\pi\sigma^2}} \times \left(\frac{SM}{M_{avg}}\right)^{\frac{1}{2m}} \exp\left\{-\frac{1}{2\sigma^2}\left[\left(\frac{SM}{M_{avg}}\right)^{\frac{1}{2m}} - a\right]^2\right\}$

Table 11. Parameters for Type IIB root normal size distributions which ensure the correct D_{avg} and M_{avg}.

a	$\sigma^2 + a^2 + \frac{2\sigma a}{\sqrt{2\pi}} \frac{\exp(-a^2/2\sigma^2)}{\mathrm{erfc}(-a/\sqrt{2}\sigma)} = 1$ (implicit equation)
A	$\mathrm{erfc}\left(-\frac{a}{\sqrt{2}\sigma}\right)$
B	$\frac{1}{\sqrt{2\pi\sigma^2}} \int_0^\infty x^{m-1/2} \exp\left[-\frac{(\sqrt{x}-a)^2}{2\sigma^2}\right] dx$
S	$a^6 + 15a^4\sigma^2 + 45a^2\sigma^4 + 15\sigma^6 + (a^4 + 14a^2\sigma^2 + 33\sigma^4)\frac{2\sigma a}{\sqrt{2\pi}} \exp\left(-\frac{a^2}{2\sigma^2}\right) \Big/ \mathrm{erfc}\left(-\frac{a}{\sqrt{2}\sigma}\right)$

For Type I root normal size distributions, f and F suffer from a severe (non-integrable) singularity at the origin. Thus most prior treatments work exclusively with f_M and F_M, which have only a mild (integrable) singularity at the origin. However, a better approach is to substitute closely-matched Type II for Type I root normal size distributions, as described by Laney (2015a).

For Type IIB root normal size distributions, there are useful analytical expressions for integer m. For example, if $m = 3$ then:

$$F_M(M) = \frac{1}{B}(a^6 + 15a^4\sigma^2 + 45a^2\sigma^4 + 15\sigma^6)\,\mathrm{erfc}\left\{\frac{1}{\sqrt{2}\sigma}\left[\left(\frac{SM}{M_{avg}}\right)^{1/6} - a\right]\right\}$$

$$+\frac{2\sigma}{\sqrt{2\pi}B}\left[\left(\frac{SM}{M_{avg}}\right)^{\frac{5}{6}} + a\left(\frac{SM}{M_{avg}}\right)^{\frac{2}{3}} + (a^2 + 5\sigma^2)\left(\frac{SM}{M_{avg}}\right)^{\frac{1}{2}}\right.$$

$$+(a^3 + 9a\sigma^2)\left(\frac{SM}{M_{avg}}\right)^{\frac{1}{3}} + (a^4 + 12a^2\sigma^2 + 15\sigma^4)\left(\frac{SM}{M_{avg}}\right)^{\frac{1}{6}}$$

$$\left. + a^5 + 14a^3\sigma^2 + 33a\sigma^4\right]\exp\left\{-\frac{1}{2\sigma^2}\left[\left(\frac{SM}{M_{avg}}\right)^{\frac{1}{6}} - a\right]^2\right\}$$

where:

$$B = (a^6 + 15a^4\sigma^2 + 45a^2\sigma^4 + 15\sigma^6)\,\mathrm{erfc}\left(-\frac{a}{\sqrt{2}\sigma}\right)$$
$$+ (a^4 + 14a^2\sigma^2 + 33\sigma^4)\frac{2\sigma a}{\sqrt{2\pi}}\exp\left(-\frac{a^2}{2\sigma^2}\right)$$

and:

$$S = a^4 + 14a^2\sigma^2 + 33\sigma^4 - 2a^2\sigma^4 - 18\sigma^6$$

4. Solid vs. Liquid: Fragment Size Distributions

Table 12 shows proposed correspondences between various solid and liquid fragment size distributions. Appendix A provides additional details for selected cases. While the type varies in the original sources, the distributions were converted to Type II or IV in all cases, with the original distributions noted in parentheses. While the fragmentation dimension *m* varies in the original sources, the distributions were converted to $m = 3$ in all cases. After making these two conversions, the proposed correspondences were chosen based solely on R_M.

Based on Table 12, the same size distribution, or nearly so, may occur for a wide range of different fragmentation events. Table 12 is not intended to be a complete listing of all possible size distributions. For example, for fragmentation of undulating liquid sheets, Bremond et. al. (2007) found a Type II Gamma size distribution with $b = 70$. Judging by R_M, this corresponds to a Type II Weibull size distribution with $n/m = 3$. For another example, for fragmentation of metal rings, Moxnes & Børve (2015) found a Type II Weibull size distribution with $n/m \approx 4$.

In Table 12, the fragment size distributions given in the white cells are approximations based on test or computational data, while those given in the grey cells are exact values derived from theory. As seen in Appendix A, the three main types of theories used are as follows:

- *Geometry, a.k.a., perfect (void free) packing theory.* If adjacent fragments meet at single point, the result has an inherently fractal character, e.g., Apollonian sphere packing. If adjacent fragments meet along extended lines or surfaces – so that the parts to fit together to form the whole like jigsaw puzzle pieces as in Lesh et. al. (2004) – the result is known as *tessellation* or *subdivision*.
- *Maximum entropy theory*. According to Englman (1996), this approach “predicts that the ‘best’ probability $p(s)$ for the occurrence of the value *s* for a variable is obtained by maximizing the information entropy subject to constraints.”
- *Governing equations* including the Population Balance Equation (PBE) and the Discrete Element Method (DEM). Both the PBE and DEM concern collections of pre-existing particles. The PBE assumes that particle properties change due to discrete events, e.g., random collisions. The DEM assumes that particle properties change due to discrete events and/or hypothetical interparticle forces. The PBE is simple enough to allow for a number of exact analytical solutions.

Table 12. Proposed correspondences between solid and liquid fragment size distributions. The white cells are approximate values based on test or computation. The grey cells are exact values based on theory.

Solids		Liquids		
Weibull	**Gamma**	**Weibull**	**Gamma**	**Root Normal**
Zhou et al. (2006) Type II $n/m = 2$ $R_M = 1.026$	Ferenc & Néda (2007) Type IVB $b = 5$ $R_M = 1.025$			Chou & Faeth (1998) Type IIB (IA) $\sigma = 0.086$ (0.081) $R_M = 1.027$ (1.02)
Cheong et al. (2003, 2004) Type II (I) $n/m = 1.5$ (2.38) $R_M = 1.049$ (1.033)			Villermaux (2007) Type IIB $b = 17$ $R_M = 1.053$	Sallam et.al. (2006) Type IIB (IA) $\sigma = 0.125$ (0.11) $R_M = 1.052$ (1.04)
Grady & Kipp (1985) Type II $n/m = 1$ $R_M = 1.075$		Li & Tankin (1987) Type II $n/m = 1$ $R_M = 1.075$	Bremond & Villermaux (2006) Type IIB $b = 10$ $R_M = 1.083$	
Grady et.al. (2001) Type II $n/m = 0.85$ $R_M = 1.094$			Marmottant & Villermaux (2004a) Type IIB $b = 8.1$ $R_M = 1.125$	
Grady et.al. (2001) Type II $n/m = 0.67$ $R_M = 1.132$			Marmottant & Villermaux (2004a) Type IIB $b = 6$ $R_M = 1.125$	Wu et. al. (1991) Type IIB (IA) $\sigma = 0.24$ (0.17) $R_M = 1.135$ (1.1)
Grady et.al. (2001) Type II $n/m = 0.55$ $R_M = 1.171$			Marmottant & Villermaux (2004b) Type IIB $b = 3.8$ $R_M = 1.172$	
Mott & Linfoot (1943) Type II $n/m = 1/2$ $R_M = 1.194$			Marmottant & Villermaux (2004b) Type IIB $b = 2.81$ $R_M = 1.208$	Empie et.al. (1995, 1997) Type IIB (IA) $\sigma = 0.34$ (0.20) $R_M = 1.195$ (1.15)
Cohen (1981) Type II $n/m = 0.433$ $R_M = 1.238$			Mulmule et.al. (2010) Type IIB $b = 2.2$ $R_M = 1.238$	Simmons (1977) Type IIB (IA) $\sigma = 0.47$ (0.238) $R_M = 1.253$ (1.2)

Table 12 ***(continued)***

Solids		Liquids		
Weibull	**Gamma**	**Weibull**	**Gamma**	**Root Normal**
Mott & Linfoot (1943) Type II $n/m = 1/3$ $R_M = 1.333$		Marshall & Palmer (1948) Type II (*) $n/m = 1/3$ $R_M = 1.333$		Spielbauer et. al. (1989) Type IIB (IA) $\sigma = 0.72$ (0.286) $R_M = 1.333$ (~1.5)

(*) Maximum entropy proof given by Cousin et. al. (1996).

In most cases, the PBE and especially DEM must be solved computationally. For example, Wittel et. al. (2004, 2005, 2006) describe a DEM approach for solid shell fragmentation based on "pointlike material elements [with] …bonds between nodes … assumed to be springs having linear elastic behavior up to failure." For another example, Carmona et. al. (2008) and Wittell et. al. (2008) describe a DEM approach for solid volumetric fragmentation based on "an agglomeration of spheres of two different sizes …connected by beam-truss elements that can elongate, shear, bend and torque," including beam breakage due to bending and stretching, and "contact forces from sphere-sphere contacts." Using this approach, Carmona et. al. (2008) and Wittell et. al. (2008) found a Weibull size distribution with $n/m \approx 2$.

In the third row of Table 12, notice that Grady & Kipp (1985) and Li & Tankin (1987) used the same approach – maximum entropy theory – to derive the same fragment size distribution within two years of each other. Grady & Kipp (1985) is well-known in the solid fragmentation community but essentially unknown in the liquid fragmentation community. Similarly, Li & Tankin (1987) is well-known in the liquid fragmentation community but essentially unknown in the solid fragmentation community.

In the last row of Table 12, notice that Mott & Linfoot (1943) and Marshall & Palmer (1948) used the same approach – curve fits to experimental data – to derive the same fragment size distribution within five years of each other. Mott & Linfoot (1943) is considered a classic in the weapons effects community; see also Grady (2006). While it is widely used to predict fragments sizes for metal-cased high-explosives, it is rarely used for other applications. Similarly, Marshall & Palmer (1948) is considered a classic in the meteorological community. While it is widely used to predict raindrop sizes, it is rarely used other applications.

Because they are based on curve fits to experiments with finite sample sizes, Weibull exponents such as $n/m = 1/2$ arguably reflect a bias toward simple rational numbers. The actual values could be slightly different. This observation is counterbalanced by the fact that at least two such rational numbers, $n/m = 1$ and $n/m = 1/3$, have been proven to be exactly correct; see Appendix A.3 and A.7. In addition, it is remarkable that different researchers working with different families of size distributions have independently arrived at such similar results. This includes Gamma and root normal size distributions whose parameters tend not to be simple rational numbers.

5. Solid vs. Liquid: Average Fragment Sizes

The size distributions seen in Sections 4 and 5 have two free parameters. This section describes a method for predicting one of those two free parameters, namely, the average fragment size. For an expanding cylindrical solid, Mott & Linfoot (1943) derived the following expression for an (unspecified) average fragment size:

$$\left(\frac{24R^2\Gamma}{\rho U^2}\right)^{1/3} \tag{12}$$

where R is the initial outer radius measured in units such as cm, Γ is the surface energy per unit area of new fragment surfaces measured in units such as dyne/cm, ρ is the density measured in units such as g/cm^3, and U is the radial expansion speed measured in units such as cm/s.

Building on Mott & Linfoot (1943), Grady (1982) suggested the following:

$$\Gamma = \sigma \tag{13}$$

for inviscid liquids where σ is the surface tension measured in units such as g/s^2 and:

$$\Gamma = \frac{K_c^2}{2\rho c_s^2} \tag{14}$$

for brittle solids where K_c is the fracture toughness measured in units such as g/(cm$^{1/2}$s^2) and c_s is the elastic wave velocity measured in units such as cm/s.

Equation (12) is derived by assuming that kinetic energy in converted to surface energy and, optionally, elastic potential energy. The derivation assumes the rate-of-strain is steady, uniform, and large. Zhou et. al. (2006) compares results from several competing theories, which gives a sense for how large the rate-of-strain needs to be; see also Grady (1988), Grady & Kipp (1993), Grady & Olsen (2003), Grady (2006), and Grady (2015).

For primary breakup of an expanding cylindrical liquid jet, Wu et. al. (1992) and Wu & Faeth (1993) found the following expression:

$$\frac{D'_{M\,avg}}{\Lambda} = \text{const.}\left(\frac{x}{\Lambda We^{1/2}}\right)^{2/3} \tag{15}$$

where:

$$We = \frac{\rho V^2 \Lambda}{\sigma}$$

is a unitless Weber number, Λ is a "radial integral length scale" comparable to the largest turbulent eddies, x is the streamwise distance along the jet, and V is the average streamwise velocity of the jet. Equation (15) can be simplified as follows:

$$D'_{M\ avg} = \text{const.}\left(\frac{\sigma x^2}{\rho V^2}\right)^{1/3} \tag{16}$$

Notice that Equations (12) and (16) are the same provided that $\Gamma = \sigma$, the unspecified average in Equation (12) is equal to the Sauter mass mean diameter, and:

$$R = \text{const.}\, x$$

$$U = \text{const.}\, V$$

Both of these are true for linearly-expanding cylindrical jets.

While Mott & Linfoot (1943) and Grady (1982) are considered to be classics in weapons effects community, they are essentially unknown in the liquid fragmentation community. Similarly, while Wu et. al. (1992) and Wu & Faeth (1993) are well-known in the atomization and sprays community, they are essentially unknown in the solid fragmentation community.

6. Solid vs. Liquid: Most Common Fragment Size Distributions

While Grady's law can be used to predict one of the free parameters in Weibull, Gamma, and root normal size distributions, there is no known method for predicting the other free parameter. As a result, fragmentation is a long-term unsolved problem.

The simplest and best-known technique relies on empirical observations. For example, for expanding solid cylinders, Mott & Linfoot (1943) suggested that the two most common fragment size distributions are Type II Weibull size distributions with:

$$n/m = 1/2$$

and

$$n/m = 1/3\,.$$

As another example, for expanding cylindrical liquid jets, Simmons (1977) suggested that the most common fragment size distribution is a Type IA root normal size distribution with:

$$\sigma = 0.238$$

As seen in Table 12, this corresponds to a Type II Weibull size distribution with:

$$n/m \approx \frac{1/2 + 1/3}{2} = 0.41667$$

In other words, the Simmons size distribution for liquid fragmentation is essentially an arithmetic average of the two Mott-Linfoot size distributions for solid fragmentation.

The Mott-Linfoot and Simmons size distributions represent large to very large fragment size spreads. However, modern designs tend to favor smaller fragment size spreads. For example, for explosively-driven metal cylinders, Grady et. al. (2001) obtained four Type II Weibull size distributions with n/m equal to 0.55, 0.67, 0.67, and 0.85. Only the first of these is anything like a Mott-Linfoot or Simmons size distribution. For another example, in a literature survey by Pimentel et. al. (2010), all of the spray systems tested prior to Simmons (1977) approximately obtained the Simmons or Mott-Linfoot size distributions; however, none of the spray systems tested afterwards did. In fact, as in seen in Table 13, the more recent the spray system, the smaller the size spread tends to be. (Remember that the size spread increases as σ increases and decreases as n/m increases.) The modern trend toward small size spreads has reduced the practical value of the Mott-Linfoot and Simmons size distributions.

Table 13a. Parameters *n/m* in a Type II Weibull and σ in Type IA root normal size distributions for spray systems measured before Simmons (1977). Based on a literature survey done by Pimentel et. al. (2010); see Laney (2015a).

n/m	σ	**Reference(s)**	**Liquid**	**Spray System**	**No.**	**%**
1/2	0.20	Turner & Moulton (1953)	β-naphthol	Swirl Jet	4	50%
0.417	0.238	Tate & Olson (1962) Houghton (1941)	Water (unknown)	Solid, Hollow Cone (unknown)	3 1	50%

Table 13b. Parameters *n/m* in a Type II Weibull and σ in Type IA root normal size distributions for sprays systems measured after Simmons (1977). Based on a literature survey done by Pimentel et. al. (2010); see Laney (2015a).

n/m	σ	**Reference(s)**	**Liquid**	**Spray System**	**No.**	**%**
2	0.081	Pimentel et. al. (2010)	Jet Fuel	'Delavan'	3	10%
3/2	0.11	Pimentel et. al. (2010) ″ ″	Jet Fuel ″ ″	'Bosch' 'BETE' 'Delavan'	4 9 1	45%
2/3	0.17	Pimentel et. al. (2010) Paloposki & Fagerholm (1986) Li & Tankin (1987) Tishkoff (1979)	(unknown) Fuel Oil Water Water	'LaVision' Hollow Cone Solid Cone Hollow Cone	3 5 4 2	45%

The Kuz-Ram method provides an empirical expression for *n* in a Type I Weibull size distribution, e.g., Cunningham (2005), Gheibie et. al. (2009). Unfortunately, this empirical expression depends on parameters specific to explosive rock mining such as borehole diameters, lengths, and spacings. There is no readily apparent extension to other applications.

7. Conclusions

In most cases, the vast majority of evidence for any given fragment size distribution is experimental. Given factors such as limited sample sizes, measurement errors, and artificial minimum fragment sizes, this leads to questions about the accuracy of any proposed fit, e.g., Clauset et. al. (2009). However, within these limitations, solid and liquid fragment size distributions often appear to be similar or identical, except possibly for extremely large or small fragments. Theories and models provide additional confirmatory evidence in selected cases.

Previous treatments of fragment size distributions often vary two or even three free parameters. However, this treatment varies only a single free parameter. Obviously, varying two or three parameters leads to significantly better agreement – with test data or with other size distributions – than varying only one parameter. However, this agreement comes at a cost, namely, such distributions may lack critical transformation and self-similarity properties, as described in Laney (2015a,b). It is unfair to compare a fit constrained by transformation and/or self-similarity properties against an unconstrained fit. The latter will inevitably appear to perform better, as judged by the usual error metrics, than the former.

Solids and liquids tend to fragment in entirely different ways. In particular, solids typically fragment via crack propagation while liquids typically fragment via hydrodynamic instability, followed by secondary breakup and coagulation. However, this work has shown that the final results are often strikingly similar. This implies that it may be unnecessary or even counterproductive to use first-principles fragmentation models, i.e., methods that accurately track the time-evolution of crack propagation or hydrodynamic instability. Indeed, such approaches still have limited predictive capability despite decades of effort. This also implies that increased interactions between the solid and liquid fragmentation communities would be mutually beneficial, e.g., it might avoid the duplication of effort seen repeatedly in the historical record.

This paper has been mainly observational. Future work will explain why manifestly different fragmentation events may produce such similar results.

References

N. Ashgriz, Editor, *Handbook of Atomization and Sprays: Theory and Applications*, Springer, 2011

J. G., Bennett, Broken Coal, *Journal of the Institute of Fuel*, 10, 22–39, 1936

N. Bremond and E. Villermaux, Atomization by Jet Impact, *Journal of Fluid Mechanics*, 549, 273-306, 2006

N. Bremond, C. Clanet, and E. Villermaux, Atomization of Undulating Liquid Sheets, *Journal of Fluid Mechanics*, 585, 421-456, 2007

W. K. Brown and K. H. Wohletz, Derivation of the Weibull Distribution Based on Physical Principles and Its Connection to the Rosin–Rammler and Lognormal Distributions, *Journal of Applied Physics*, 78(4), 2758-2763, 1995

H. A. Carmona, F. K. Wittel, F. Kun, and H. J. Herrmann, Fragmentation Processes in Impact of Spheres, *Physical Review E*, 77, 051302, 2008

Y. S. Cheong, A. D. Salman, and M. J. Hounslow, Effect of Impact Angle and Velocity on the Fragment Size Distribution of Glass Spheres, *Powder Technology*, 138, 189-200, 2003

Y. S. Cheong, G. K. Reynolds, A. D. Salman, and M. J. Hounslow, Modelling Fragment Size Distribution using Two-Parameter Weibull Equation, *International Journal of Mineral Processing*, 74S, S227-S237, 2004

W.-H. Chou and G. M. Faeth, Temporal Properties of Secondary Drop Breakup in the Bag Breakup Regime, *International Journal of Multiphase Flow*, 24, 889-912, 1998

A. Clauset, C. R. Shalizi, and M. E. J. Newman, Power-Law Distributions in Empirical Data, *SIAM Review*, 51(4), 661–703, 2009

E. A. Cohen, New Formulas for Predicting the Size Distribution of Warhead Fragments, *Mathematical Modeling*, 2, 19-32, 1981

C. V. B. Cunningham, The Kuz-Ram Fragmentation Model – 20 Years On, In R. Holmberg et. al., Editors, *Proceedings of the 3rd World Conference on Explosives and Blasting*, EFEE, 2005

H. J. Empie, S. J. Lien, W. Yang, and T. N. Adams, Spraying Characteristics of Commercial Black Liquor Nozzles, *TAPPI Journal*, 78(1), 121-128, 1995

H. J. Empie, S. J. Lien, and W. Yang, Drop Size Modification in Black Liquor Sprays From Commercial Nozzles Using Pulsed Flow, *Atomization and Sprays*, 7, 457-466, 1997

R. Englman, Maximum Entropy Principles in Fragmentation Data Analysis, In L. Davison, D. E. Grady, and M. Shahinpoor, Editors, *High-Pressure Shock Compression of Solids II*, Springer-Verlag, 1996

J.-S. Ferenc and Z. Néda, On the Size Distribution of Poisson Voronoi Cells, *Physica A*, 385(2), 518-526, 2007

S. Gheibie, H.Aghababaei, S.H.Hoseinie, and Y.Pourrahimian, Modified Kuz-Ram Fragmentation Model and its use at the Sungun Copper Mine, *International Journal of Rock Mechanics and Mining Sciences*, 46, 967–973, 2009

D. E. Grady, Local Inertial Effects in Dynamic Fragmentation, *Journal of Applied Physics*, 53(1), 322-325, 1982

D. E. Grady and M. E. Kipp, Geometric Statistics and Dynamic Fragmentation, *Journal of Applied Physics*, 58(3), 1985

D. E. Grady and M. E. Kipp, Dynamic Rock Fragmentation, In B. K. Atkinson, Editor, *Fracture Mechanics of Rock*, Academic Press, 429-475, 1987

D. E. Grady, The Spall Strength of Condensed Matter, *Journal of Mechanics and Physics of Solids*, 36(3), 353–384, 1988

D. E. Grady and M. E. Kipp, Dynamic Fracture and Fragmentation, In J. R. Asay and M. Shahinpoor, Editors, *High-Pressure Shock Compression of Solids*, Springer-Verlag, 1993 (see also D. E. Grady and M. E. Kipp, Fragmentation of Solids Under Dynamic Loading, in T. Wierzbicki and N. Jones, Editors, *Structural Failure*, Wiley, 1989)

D. E. Grady, L. T. Wilson, D. R. Reedal, L. D. Kuhns, M. E. Kipp, and J. W. Black, Comparing Alternate Approaches in the Scaling of Naturally Fragmenting Munitions, In I. R. Crewther, Editor, *Proceedings of the 19th International Symposium on Ballistics*, IBS, 2001

D. E. Grady and M. L. Olsen, A Statistics and Energy Based Theory of Dynamic Fragmentation, *International Journal of Impact Engineering*, 29, 293-306, 2003

D. E. Grady, *Fragmentation of Rings and Shells: The Legacy of N. F. Mott*, Springer, 2006

D.E. Grady, The Unifying Role of Dissipative Action in the Dynamic Failure of Solids, *Procedia Engineering*, 103, 143-150, 2015

L. Griffith, A Theory of the Size Distribution of Particles in a Comminuted System, *Canadian Journal of Research*, 21A(6), 1943

L.-P. Hsiang and G. M. Faeth, Near-Limit Drop Deformation and Secondary Breakup, *International Journal of Multiphase Flow*, 18(5), 635-652, 1992

C. B. Laney, *Improved Root Normal Size Distributions for Liquid Atomization*, Defense Threat Reduction Agency Technical Report DTRA-TR-16-003, November 2015

C. B. Laney, *Transformation and Self-Similarity Properties of Gamma and Weibull Fragment Size Distributions*, Defense Threat Reduction Agency Technical Report DTRA-TR-16-006, December 2015

N. Lesh, J. Marks, A. McMahon, and M. Mitzenmacher, Exhaustive Approaches to 2D Rectangular Perfect Packings, *Information Processing Letters*, 90, 7-14, 2004

X. Li and R. S. Tankin, Droplet Size Distribution: A Derivation of a Nukiyama-Tanasawa Type Distribution Function, *Combustion Science and Technology*, 65–76, 1987

H. Liu, *Science and Engineering of Droplets: Fundamentals and Applications*, William Andrew Publishing, 2000

P. Marmottant and E. Villermaux, Fragmentation of Stretched Liquid Ligaments, *Physics of Fluids*, 16(8), 2732-2741, 2004a

P. Marmottant and E. Villermaux, On Spray Formation, *Journal of Fluid Mechanics*, 498, 73-111, 2004b

J. S. Marshall and W. M. Palmer, The Distribution of Raindrops with Size, *Journal of Meteorology*, 5(4), 165–166, 1948

Z. A. Melzak, The Effects of Coalescence in Certain Collision Processes, *Quarterly Journal of Applied Mathematics*, 11, 231–236, 1953

N. F. Mott and E. H. Linfoot, *A Theory of Fragmentation*, U. K. Ministry of Supply, AC3348, January 1943 [reproduced in Grady (2006)]

J. F. Moxnes and S. Børve, Simulation of Natural Fragmentation of Rings Cut from Warheads, *Defence Technology*, 11(4), Pages 319–329, 2015

A. S. Mulmule, M. S. Tirumkudulu, and K. Ramamurthi, Instability of a Moving Liquid Sheet in the Presence of Acoustic Forcing, *Physics of Fluids*, 22, 022101, 2010

T. Paloposki and N. E. Fagerholm, *The Atomization of Heavy Fuel Oil with Swirl Pressure Jet Atomizer*, Helsinki University of Technology, Institute of Energy Engineering Research Report TKK-KO/ET-13, NTIS Accession Number DE87751107, 1986

R. Pimentel, R. Stowe, P. Harris, A. DeChamplain, and D. Kretschmer, Spray Characterization Based on the Pearson System of Frequency Curves, *Atomization and Sprays*, 20(5), 365-386, 2010

P. Rosin and E. Rammler, Feinheit und Struktur des Kohlenstaubs, *Zeitschrift des Vereins Deutscher Ingenieure*,71, 1–7, 1927

P. Rosin, E. Rammler, and K. Sperling, Korngrößenprobleme des Kohlenstaubes und ihre Bedeutung für die Vermahlung, *Bericht C 52 des Reichskohlenrates*, VDI-Verlag, 1933

P. Rosin and E. Rammler, Die Kornzusammensetzung des Mahlgutes im Lichte der Wahrscheinlichkeitslehre, *Kolloid-Zeitschrift*, 67(1), 16-26, 1934

K.A. Sallam, C. Aalburg, G.M. Faeth, K.-C. Lin, C.D. Carter, and T.A. Jackson, Primary Breakup of Aerated-Liquid Jets in Supersonic Crossflows, *Atomization and Sprays*, 16(6), 657-672, 2006

H. C. Simmons, The Correlation of Drop-Size Distributions in Fuel Nozzle Spray, Parts I and II, *Transactions of the ASME, Journal of Engineering for Power*, 99, 309-319, 1977

T. M. Spielbauer, T. N. Adams, J. E. Monacelli, and R. T. Bailey, Droplet Size Distribution of Black Liquor Sprays, *Proceedings of International Chemical Recovery Conference*, Ottawa, Canada, TAPPI/CPPA, 1989

R. W. Tate and E. O. Olson, Spray Droplet Size of Pressure-Atomizing Burner Nozzles, *ASHRAE Journal*, 4(3), 39-43, 1962

J. M. Tishkoff and C. K. Law, Application of a Class of Distribution Functions to Drop-Size Data by Logarithmic Least-Squares Technique, *Transactions of the ASME, Journal of Engineering for Power*, 99A(4), 684-688, 1977

J. M. Tishkoff, *GMR Laser-video Imaging System Results for the ASTM 'Round-Robin' Nozzle Test*, General Motors Research Publication GMR-3098, 1979

G. M. Turner and R. W. Moulton, Drop Size Distributions from Spray Nozzles, *Chemical Engineering Progress*, 49(4), 185-190, 1953

E. Villermaux, P. Marmottant, and J. Duplat, Ligament-Mediated Spray Formation, *Physical Review Letters*, 92(7), 074501-2, 2004

E. Villermaux, Fragmentation, *Annual Review Fluid Mechanics*, 39, 419-446, 2007

E. Villermaux and B. Bossa, Single-Drop Fragmentation Determines Size Distribution of Raindrops, *Nature Physics*, 5, 697 – 702, 2009

W. Weibull, A Statistical Theory of the Strength of Materials, *Ingenïors Vetenskaps Akademiens Handligar*, 151, 1-45, 1939

W. Weibull, The Phenomenon of Rupture in Solids, *Ingenïors Vetenskaps Akademiens Handligar*, 153, 1-55, 1939

F. K. Wittel, F. Kun, H. J. Herrmann, and B. H. Kröplin, Fragmentation of Shells, *Physical Review Letters*, 93(3), 035504, 2004

F. K. Wittel, F. Kun, H. J. Herrmann, and B. H. Kröplin, Breakup of Shells Under Explosion and Impact, *Physical Review E*, 71(1), 016108, 2005

F. K. Wittel, F. Kun, B. H. Kröplin, and H. J. Herrmann, Study on the Fragmentation of Shells, *International Journal of Fracture*, 140, 243, 2006

F. K. Wittel, H. A. Carmona, F. Kun, and H. J. Herrmann, Mechanisms in Impact Fragmentation, *International Journal of Fracture*, 154(1-2), 105-117, 2008

P.-K. Wu, L.-K. Tseng, and G. M. Faeth, Primary Breakup in Gas/Liquid Mixing Layers for Turbulent Liquids, *Atomization and Sprays*, 295-317, 1992

P.-K. Wu, G. A. Ruff, and G. M. Faeth, Primary Breakup in Liquid-Gas Mixing Layers, *Atomization and Sprays*, 1, 421-440, 1991

P.-K. Wu and G. M. Faeth, Aerodynamic Effects on Primary Breakup of Turbulent Liquids, *Atomization and Sprays*, 3, 265-289, 1993

F. Zhou, J.-F. Molinari, and K. T. Ramesh, Characteristic Fragment Size Distributions in Dynamic Fragmentation, *Applied Physics Letters*, 88, 261918, 2006

Appendix A: Specific Examples of Solid vs. Liquid Fragment Size Distributions

A.1. Example 1

This example concerns three fragment size distributions with $R_M = 1.026 \pm 0.001$. These distributions are considered to have a very narrow size spread.

1.) Based on a literature survey of experimental results for expanding solid rings with $m = 1$, Zhou et. al. (2006) suggested the following fragment size distribution:

$$F(M) = \exp\left[-\left(\frac{M - M_{\min}}{M_{ref}}\right)^2\right] \tag{A1a}$$

$$f(M) = \frac{2}{M_{ref}^2}\left(M - M_{\min}\right)\exp\left[-\left(\frac{M - M_{\min}}{M_{ref}}\right)^2\right] \tag{A1b}$$

where $M_{\min}$ is a minimum fragment size and M_{ref} is a reference fragment size. If $M_{\min} = 0$, then by Table 3, this is a Type II Weibull size distribution with:

$$n/m = 2 \tag{A1c}$$

This particular Weibull size distribution is also known as a Rayleigh distribution. As shown by Laney (2015b), Weibull distributions are the same regardless of normalization. In other words, $n/m = 2$ regardless of whether M_{ref} is chosen to be M_{avg}, $M_{M\ avg}$, or some other average.

Zhou et. al. (2006) drew on four experimental studies. Unfortunately, all four suffered from low sample sizes, with the number of fragments varying between 18 and 125, the latter obtained only by repeating the same test 11 times. Grady and Olsen (2003) and Grady (2006) provide alternative fits, including rare applications of Mott (1947), that may better account for the effects of such small sample sizes.

2.) Based on computational results for Voronoi tessellation of unitary solid bodies with $m = 1, 2$, or 3, Ferenc & Néda (2007) suggested the following fragment size distribution:

$$f(M) = \frac{\left(\frac{3m+1}{2}\right)^{\frac{3m+1}{2}}}{M_{avg}\Gamma\left(\frac{3m+1}{2}\right)}\left(\frac{M}{M_{avg}}\right)^{\frac{3m+1}{2}-1}\exp\left[-\frac{3m+1}{2}\frac{M}{M_{avg}}\right] \tag{A2a}$$

By Table 6, this is a Type IV Gamma size distribution with:

$$b = \frac{3m+1}{2} \tag{A2b}$$

For comparison, based on earlier computational results for Voronoi tessellation for unitary solid bodies such as asteroids, Kiang (1966) suggested a Type IV Gamma size distribution with:

$$b = 2m \tag{A3}$$

Equation (A3) predicts somewhat larger values for *b* than Equation (A2) when $m > 1$.

3.) Based on experimental results for bag-type aerodynamic breakup of water droplets, Chou & Faeth (1998) suggested a Type IA root normal size distribution with $R_M = 1.02$ or equivalently:

$$\sigma \approx 0.081, \quad a = 1 \tag{A4}$$

Laney (2015a) showed that this is nearly identical to a Type IIB root normal size distribution with $R_M = 1.027$ or equivalently:

$$\sigma = 0.086, \; a = 0.9963 \tag{A5}$$

Notice that most liquid atomization events produce nearly-spherical droplets with $m = 3$. This is true even when the atomizing body is one-dimensional such a ring, ligament, or filament or two-dimensional such as a bag or sheet.

Figure A.1 shows four different views of the Type II Weibull size distribution given by Equation (A1), the Type IIB Gamma size distribution given by Equation (A2), and the Type IIB root normal size distribution given by Equation (A5). These three size distributions are compared to each other and to experimental data for liquid atomization due to Pimentel et. al. (2010) and computational data for solid fragmentation due to Wittell et. al. (2008). In the latter case, Wittell et. al. (2008) used a Discrete Element Model (DEM) to simulate 16mm-diameter polymer spheres impacting hard frictionless plates; see also Carmona et. al. (2008). The smallest fragments in Wittell et. al. (2008) appear to obey a power law. In addition, the largest liquid fragments in Pimentel et. al. (2010) appear to obey a power law. In this case, the Weibull size distribution appears to obtain somewhat better agreement with the experimental data that the Gamma and root normal distribution, which are nearly the same.

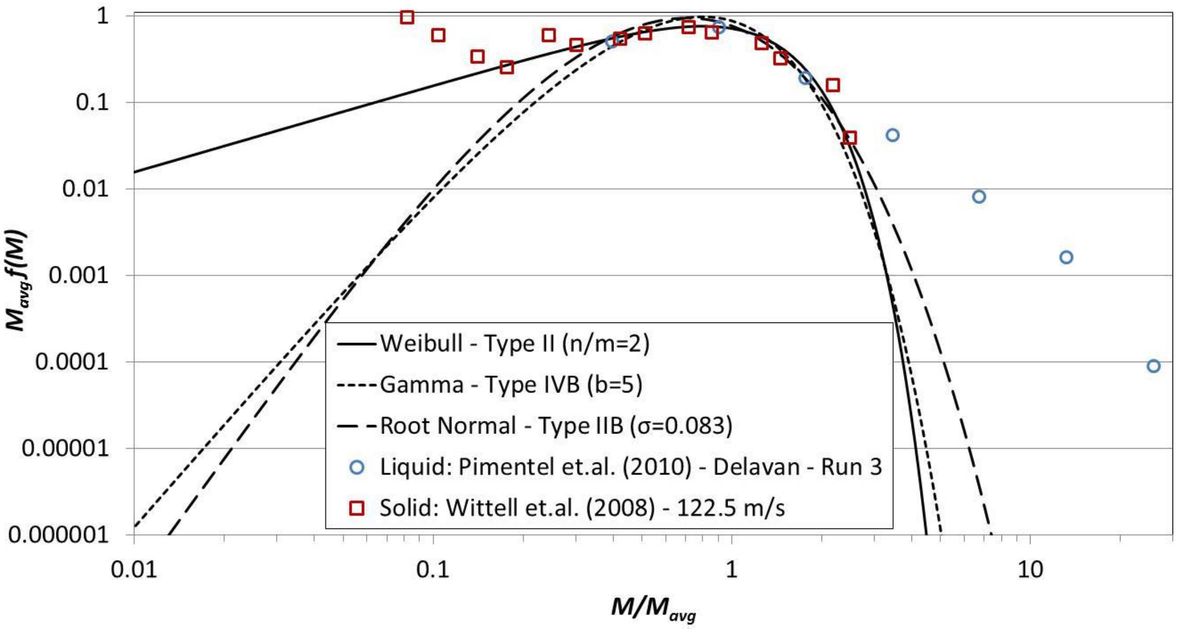

(a.) $f(M)$ in the log-log plane

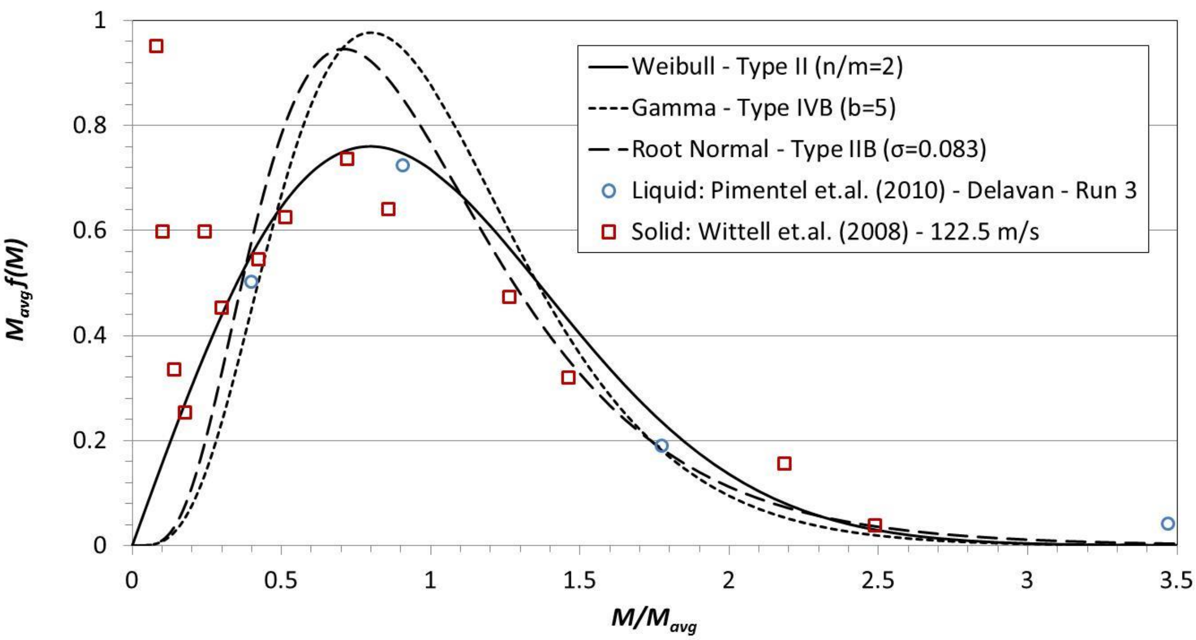

(b.) $f(M)$ in the linear-linear plane

Figure A.1. Type II Weibull, Gamma, and root normal size distributions vs. experimental data for liquid atomization due to Pimentel et. al. (2010) and computational data for solid fragmentation due to Wittell et. al. (2008). The Weibull, Gamma, and root normal size distributions all have R_M = 1.026±0.001.

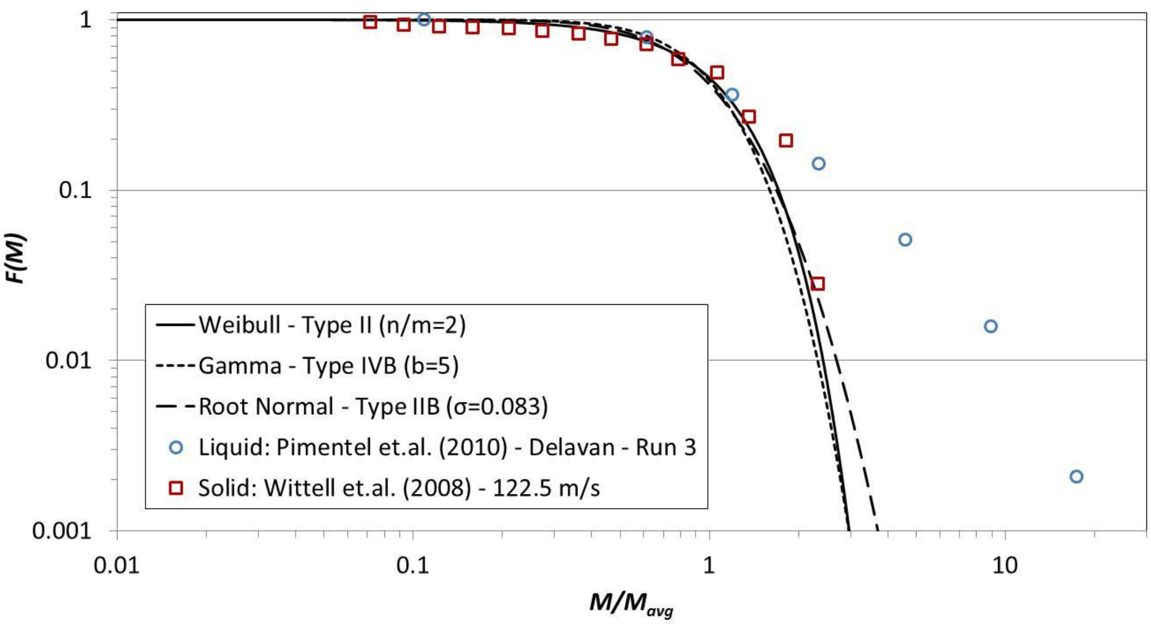

(c.) ***F*(*M*) in the log-log plane**

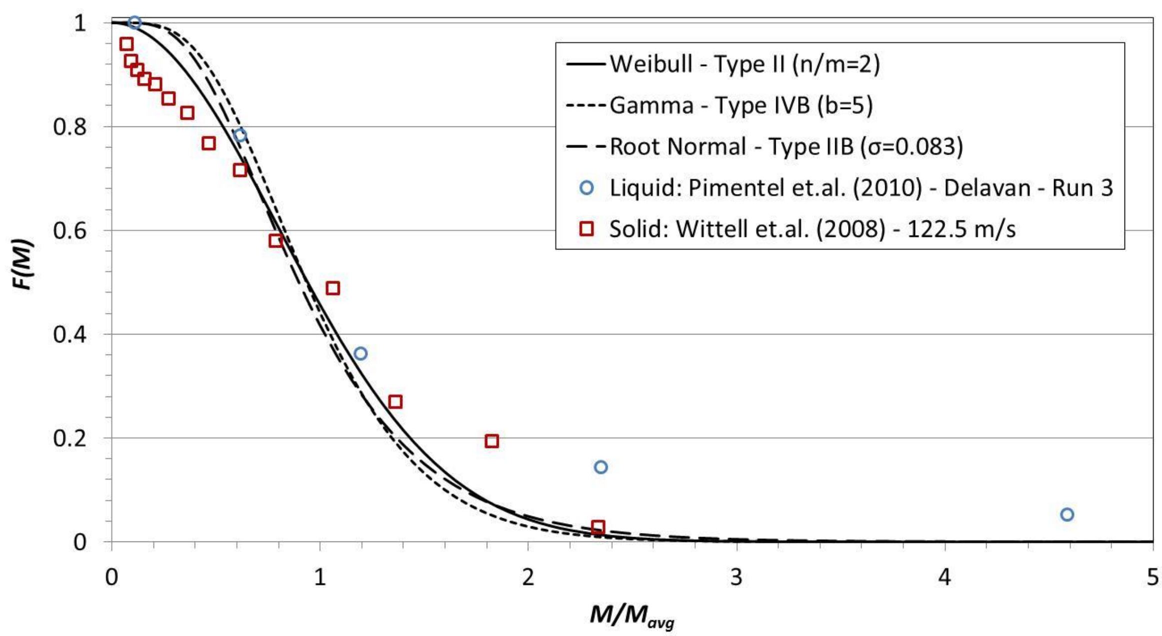

(d.) ***F*(*M*) in the linear-linear plane**

Figure A.1. ***(continued)***

A.2. Example 2

This example concerns three fragment size distributions with $R_M = 1.051 \pm 0.002$. These distributions are considered to have a narrow fragment size spread.

1.) Cheong et. al. (2003, 2004) studied gun-launched soda-lime glass spheres impacting thick aluminum oxide blocks. In these tests, fragments originated entirely from the surfaces of the spheres, leaving the interiors intact, which implies m = 2. For an impact angle of 60º, they obtained the following fragment size distributions:

$$F_M(D) = \exp[-(D/D_{ref})^n] \tag{A6a}$$

where D is "an equivalent diameter of a circle having the same area as the projected area of the corresponding fragment," D_{ref} is a reference diameter, and:

$$n = 4.76 \pm 33\% \tag{A6b}$$

is an average over four measurements. According to Table 2, this is a Type I Weibull size distribution with $n/m = 2.38$. As shown by Laney (2015b), this is approximately the same as a Type II Weibull size distribution with:

$$n/m = 1.5 \tag{A7}$$

As noted earlier, Weibull distributions are the same regardless of normalization. In other words, $n/m = 1.5$ regardless of whether D_{ref} is chosen to be D_{avg}, $D_{M\ avg}$, or some other average.

2.) Based on experimental results for fragmentation of liquid sheets, Villermaux (2007) suggested a Type IIB Gamma size distribution with:

$$b = 17 \tag{A8}$$

3.) Based on experimental results for round aerated liquid jets, Sallam et. al. (2006) suggested a Type IA root normal size distribution with $R_M = 1.04$ or equivalently:

$$\sigma \approx 0.11, \quad a = 1 \tag{A9}$$

Laney (2015a) showed that this is nearly identical to a Type IIB root normal size distribution with $R_M = 1.049$ or equivalently:

$$\sigma = 0.125,\ a = 0.9922 \tag{A10}$$

Figure A.2 shows four views of the Type II Weibull size distribution given by Equation (A7), the Type IIB Gamma size distribution given by Equation (A8), and the Type IIB root normal size distribution given by Equation (A10). These three size distributions are compared to each other

and to experimental data for liquid atomization due to Pimentel et. al. (2010). The largest liquid fragments in Pimentel et. al. (2010) appear to obey a power law. In this case, the Gamma and root normal size distributions, which are nearly the same, appear to obtain somewhat better agreement with the experimental data than the Weibull size distribution.

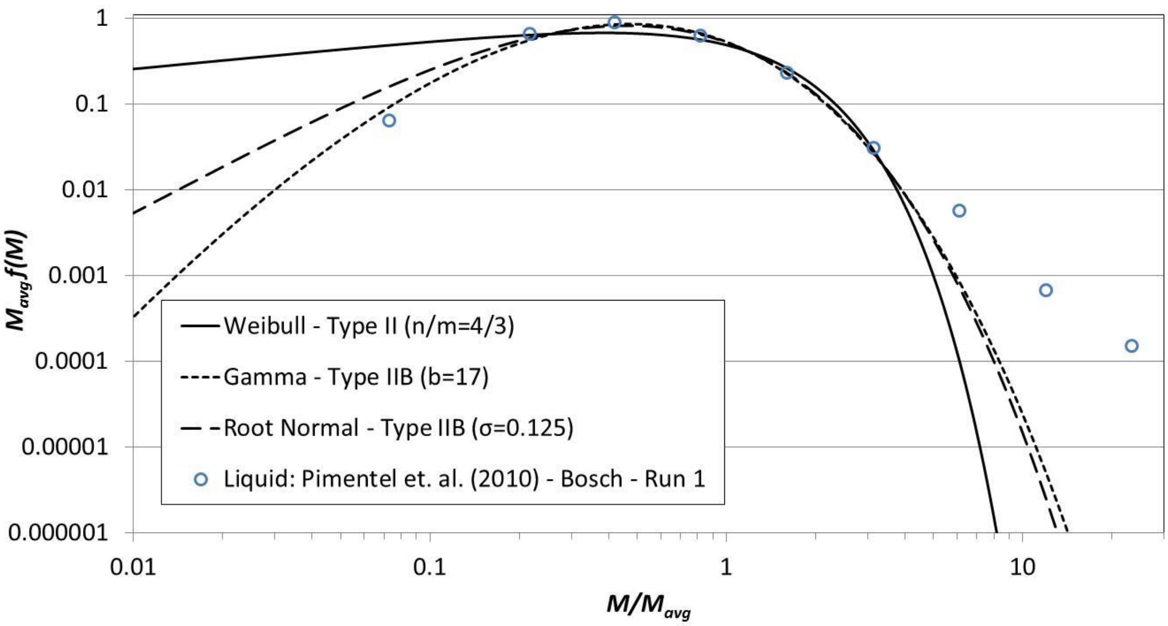

(a.) *f*(*M*) in the log-log plane

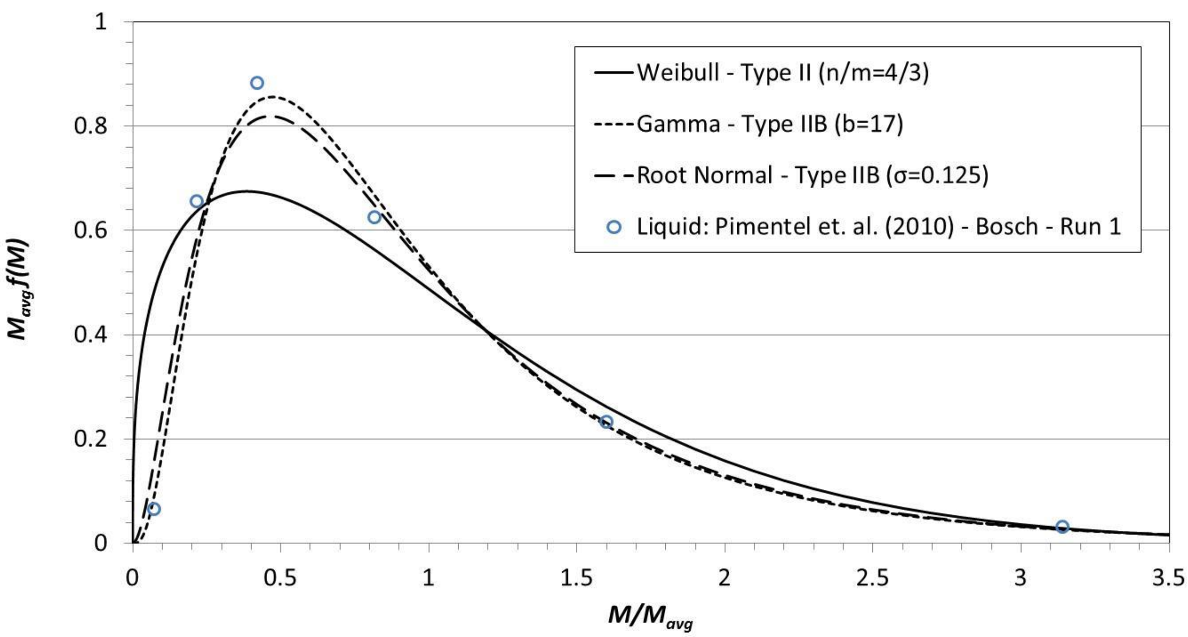

(b.) *f*(*M*) in the linear-linear plane

Figure A.2. Type II Weibull, Gamma, and root normal size distributions vs. experimental data for liquid atomization due to Pimentel et. al. (2010). The Weibull, Gamma, and root normal size distributions all have R_M = 1.051±0.002.

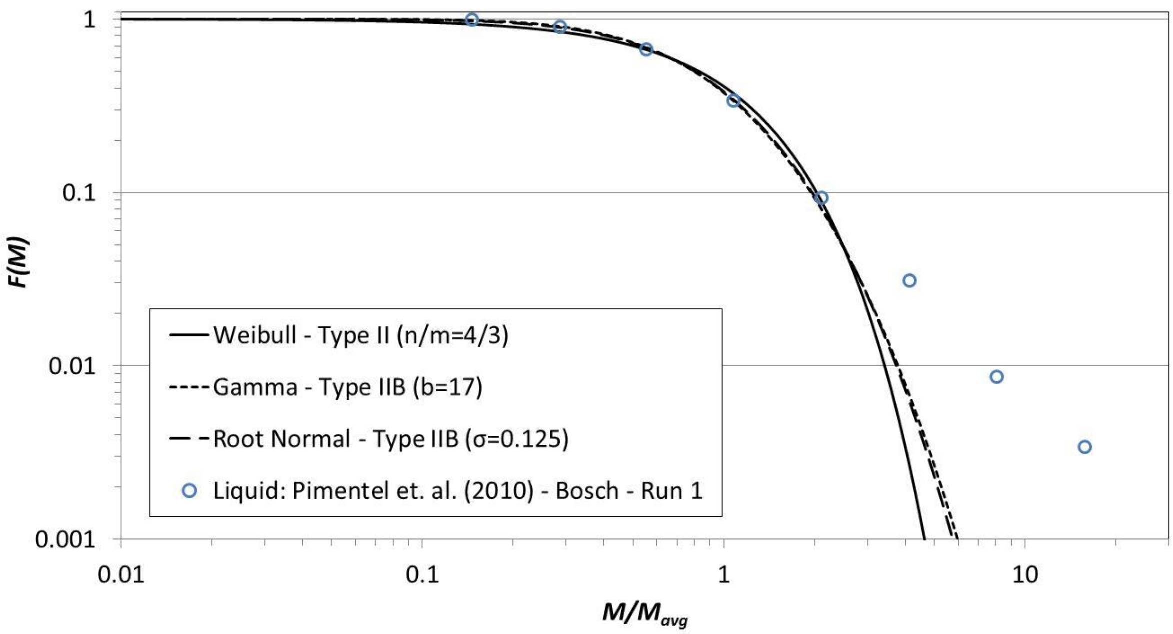

(c.) ***F*****(*****M*****) in the log-log plane**

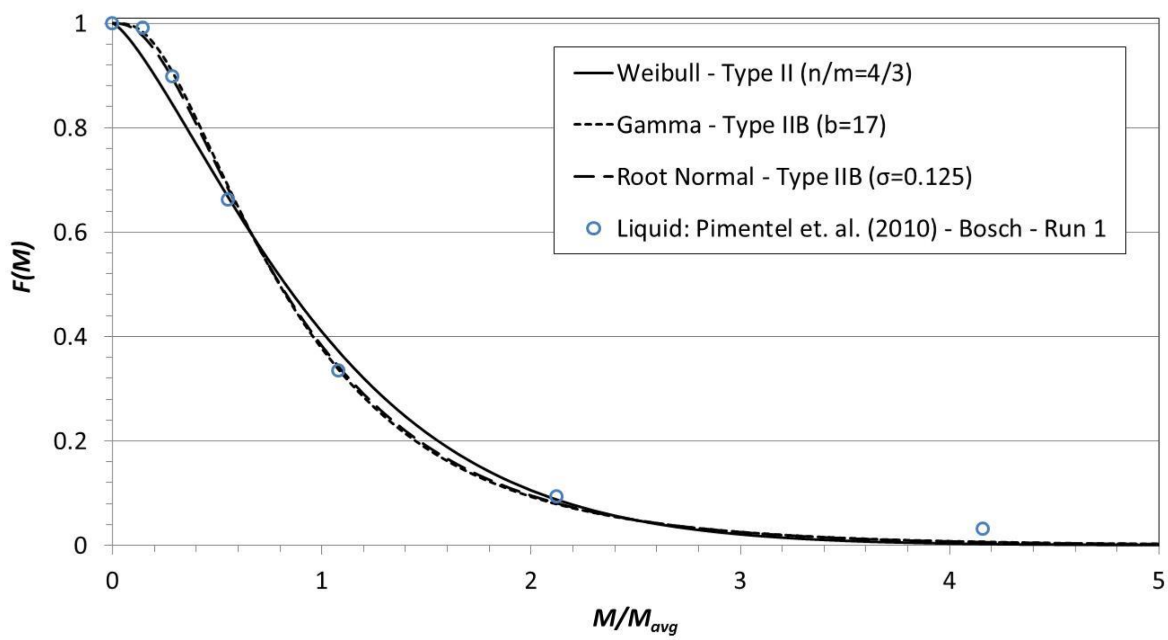

(d.) ***F*****(*****M*****) in the linear-linear plane**

Figure A.2 ***(continued)***

A.3. Example 3

This example concerns fragment size distributions with $R_M = 1.080 \pm 0.005$. These distributions are considered to have a medium-to-narrow size spread

1.) For fragmenting bodies with $m = 1$, Lineau (1936) derived the following size distribution:

$$F(M) = \exp(-\text{const.}\, M) \tag{A11a}$$

By Table 3, this is a Type II Weibull size distribution with:

$$n/m = 1 \tag{A11b}$$

As noted earlier, Weibull size distributions are the same regardless of normalization. In other words, it makes no difference that Table 3 includes M_{avg} while Equation (A11) does not.

Grady & Kipp (1985) extended Equation (A11) to solid fragmenting bodies with $m = 2$ and 3. As one proof, they used a computational method to determine the size distributions resulting from a variety of different two-dimensional subdivisions involving horizontal, vertical, and randomly-oriented line segments. In all cases considered, except for Voronoi tessellations, their computational results approximately obtained Equation (A11). More recently, Cowan (2010) proved that Equation (A11) is exact in the limit of an infinite number of iterative line-segment-based subdivisions. As another proof, Grady & Kipp (1985) derived Equation (A11) for $m = 2$ using a maximum entropy approach assuming that "every fragment has equal probability of being large or small," provided only that the total cross-sectional area is correct.

2.) Using a maximum entropy approach with $m = 3$, Li & Tankin (1987) derived the following aerosol size distribution:

$$f(D) = \frac{1}{AD_{ref}}\left(\frac{D}{D_{ref}}\right)^2 \exp\left[-a\left(\frac{D}{D_{ref}}\right)^3\right] \tag{A12a}$$

By Table 3, this is a Type II Weibull size distribution with $n = 3$ or equivalently:

$$n/m = 1 \tag{A12b}$$

As noted earlier, Weibull size distributions are the same regardless of normalization. In other words, it makes no difference that Table 3 uses D_{avg} while Equation (A12) uses D_{ref}.

3.) For collision-driven fragmentation and coagulation in a pre-existing population of liquid droplets, a number of researchers have derived the following aerosol size distribution:

$$f(M) = \frac{1}{M_{ref}} \exp\left[-\frac{M}{M_{ref}} \right] \tag{A13a}$$

By Table 3, this is a Type II Weibull size distribution with:

$$n/m = 1 \tag{A13b}$$

As noted earlier, it makes no difference that Table 3 uses M_{avg} while Equation (A13) uses M_{ref}.

Equation (A13) is derived by finding the late-time analytic limit of the Population Balance Equation (PBE). For example, Mulholland & Baum (1980) and Lehtinen & Zachariah (2001) obtained this result for droplet coagulation, while Attarakih et. al. (2004) obtained this result for droplet fragmentation. Notice that, since n/m is the same, Equations (A11), (A12), and (A13) are all the same.

4.) Based on experimental results for fragmentation of liquid sheets, Bremond & Villermaux (2006) and Villermaux (2007) suggested a Type IIB Gamma size distribution with:

$$b = 10 \tag{A14}$$

Figure A.3 compares the Type II Weibull size distribution given by Equations (A11), (A12), and (A3) to the Type II Gamma size distribution given by Equation (A14). In this case, the two size distributions are fairly similar except at the extremes.

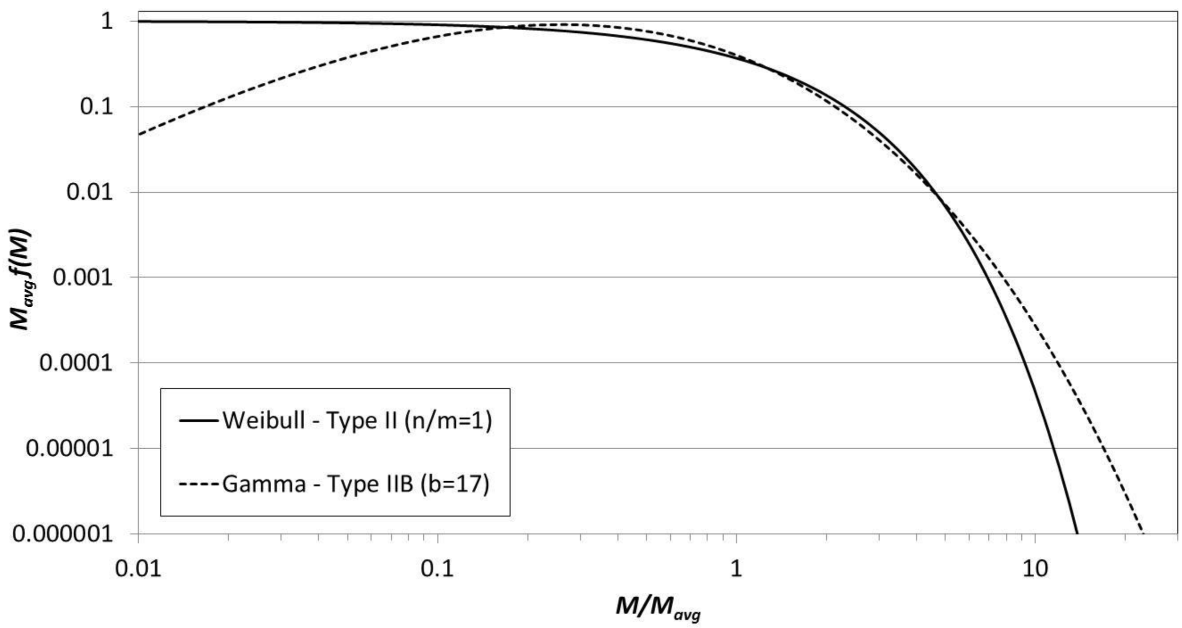

(a.) ***f*(*M*) in the log-log plane**

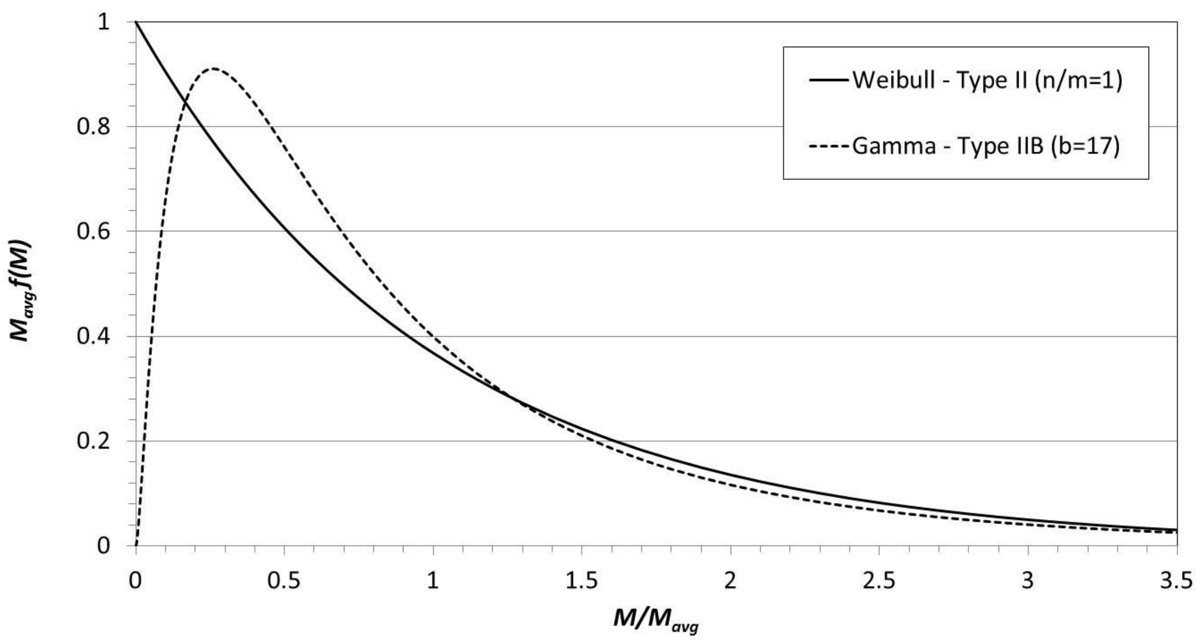

(b.) ***f*(*M*) in the linear-linear plane**

Figure A.3. Type II Weibull vs. Gamma size distributions. Both distributions have R_M = 1.08±0.005.

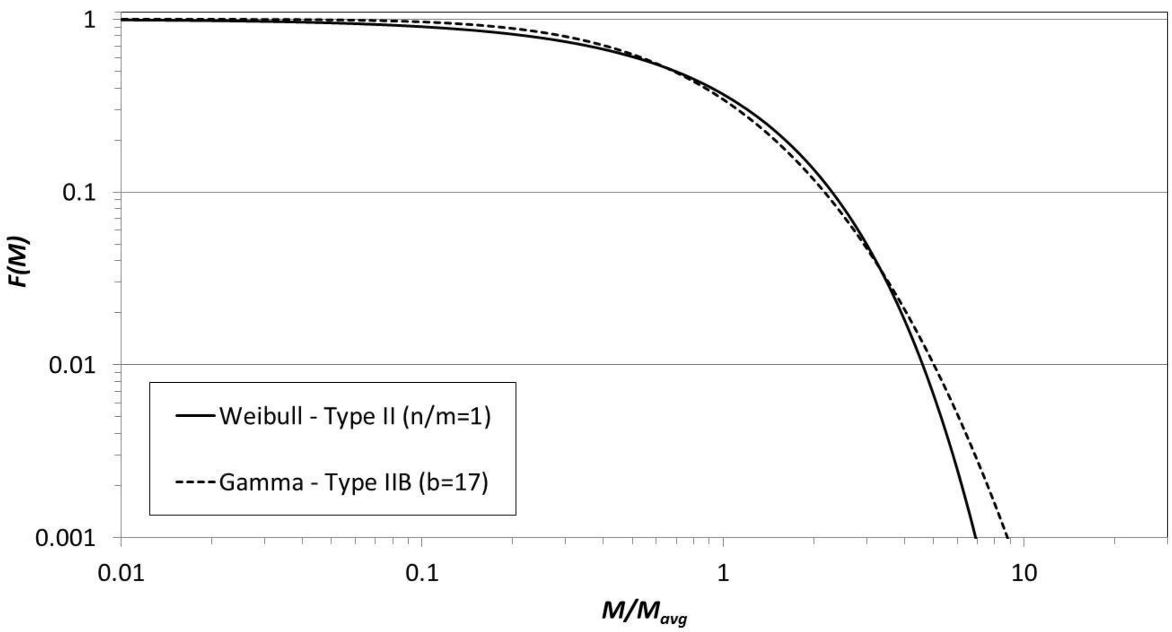

(c.) ***F*(*M*) in the log-log plane**

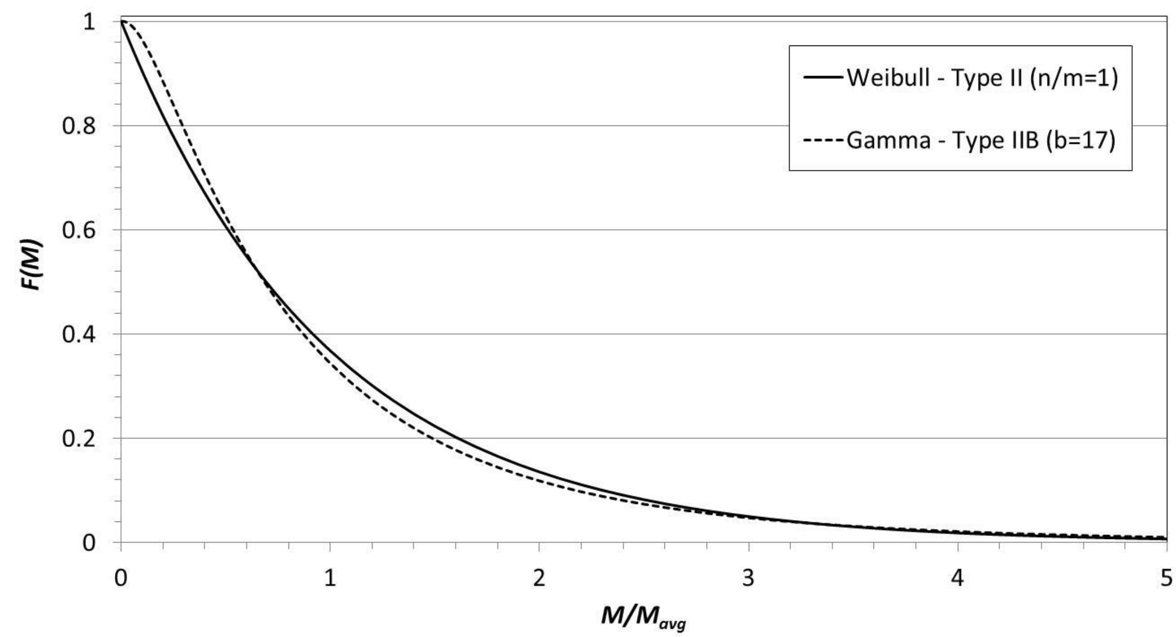

(d.) ***F*(*M*) in the linear-linear plane**

Figure A.3. ***(continued)***

A.4. Example 4

This example concerns fragment size distributions with $R_M = 1.130 \pm 0.005$. These distributions are considered to have a medium-to-wide size spread.

1.) Based on experimental data for expanding cylindrical steel shells, Grady et. al. (2001) suggested the following fragment size distribution:

$$F(M) = \exp[-(M/M_{ref})^{0.67}] \tag{A15a}$$

By Table 3, this is a Type II Weibull size distribution with:

$$n/m \approx 2/3 \tag{A15b}$$

More specifically, Grady et. al. (2001) tested cylinders with lengths of either 10cm or 20cm. In either case, the wall thickness to inner radius ratio was 0.8. For as-received steel, the longer and shorter fragmenting cylinders obtained Type II Weibull size distributions with $n/m = 0.85$ and $n/m = 0.55$, respectively. However, after heat treatment, the longer and shorter fragmenting cylinders both obtained $n/m = 0.67$.

2.) Based on experimental data for fragmentation of stretched ethanol ligaments, Marmottant & Villermaux (2004a) suggested a Type IIB Gamma size distribution with:

$$b = 6 \tag{A16}$$

3.) Based on experimental results for round liquid jets in still air, Wu et. al. (1991) suggested a Type IA root normal size distribution with $R_M = 1.1$ or equivalently:

$$\sigma \approx 0.17, \quad a = 1 \tag{A17}$$

Laney (2015a) showed that this is approximately equal to a Type IIB root normal size distribution with $R_M = 1.135$ or equivalently:

$$\sigma = 0.24, \; a = 0.9708 \tag{A18}$$

Figure A.4 shows four views of the Type II Weibull size distribution given by Equation (A15), the Type IIB Gamma size distribution given by Equation (A16), and the Type IIB root normal size distribution given by Equation (A18). These three size distributions are compared to each other and to experimental data for liquid atomization due to Li & Tankin (1987) and experimental data for solid fragmentation due to Bewick et. al. (2015). Bewick et. al. (2015) used an explosively-driven 6.5-inch-diameter shock tube to load a ¼-inch-thick glass plate to a peak overpressure of approximately 500psi. In this case, the Weibull and root normal size distributions, which are nearly the same, appear to obtain somewhat better agreement with the experimental data than the Gamma distribution.

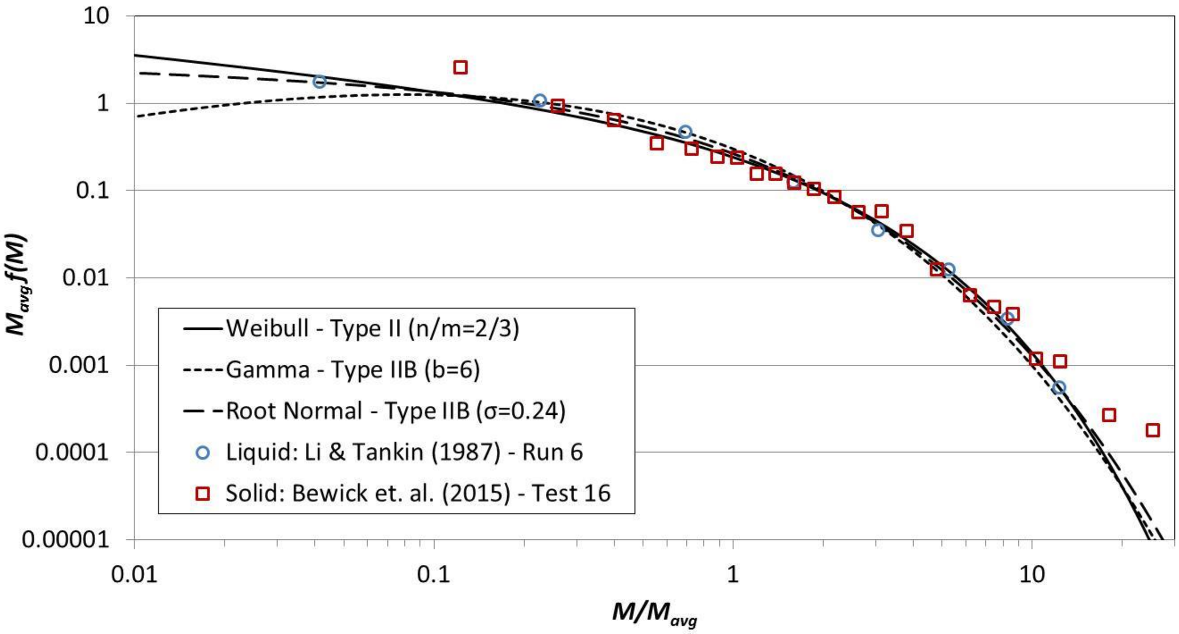

(a.) *f*(*M*) in the log-log plane

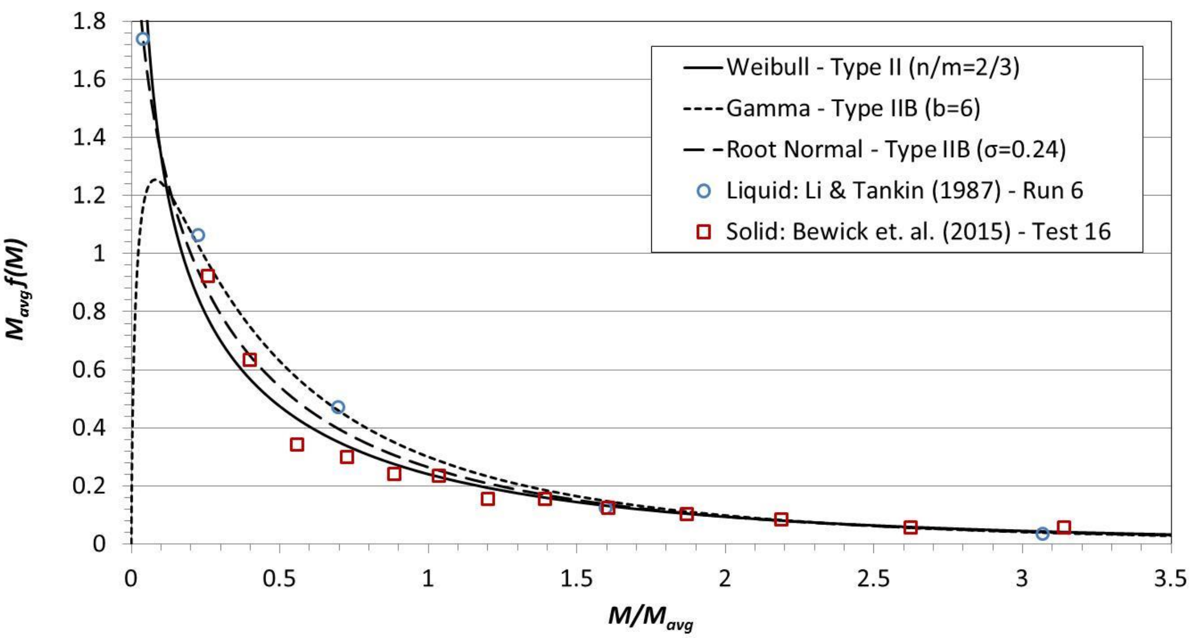

(b.) *f*(*M*) in the linear-linear plane

Figure A.4. Type II Weibull, Gamma, and root normal size distributions vs. experimental data for liquid atomization due to Li & Tankin (1987) and experimental data for solid fragmentation due to Bewick et. al. (2015). The Weibull, Gamma, and root normal size distributions all have R_M = 1.13±0.005.

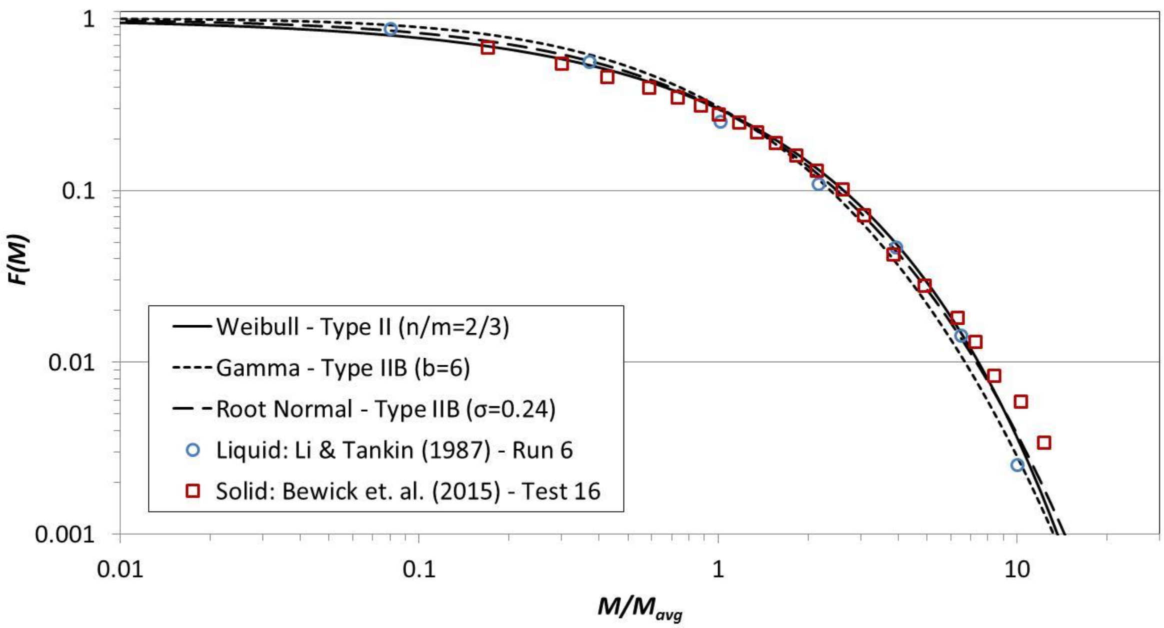

(c.) ***F*(*M*) in the log-log plane**

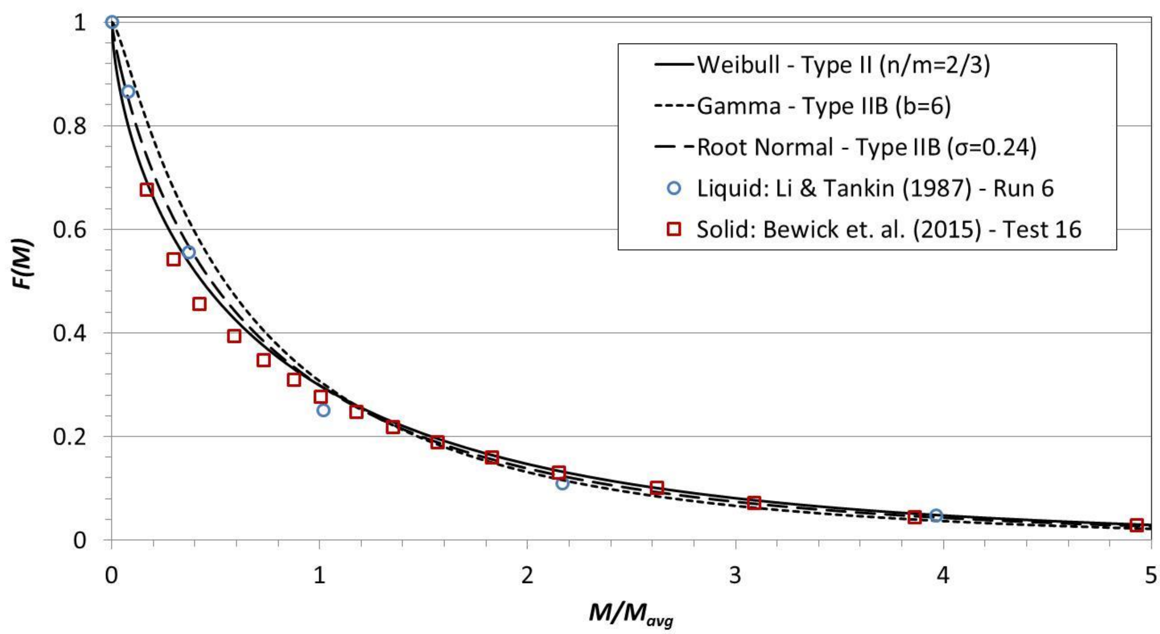

(d.) ***F*(*M*) in the linear-linear plane**

Figure A.4. ***(continued)***

A.5 Example 5

This example concerns fragment size distributions with $R_M = 1.2 \pm 0.008$. These distributions are considered to have a wide size spread.

1.) For cylindrical high-explosives detonated inside cylindrical metal shells, Mott & Linfoot (1943) suggested the following fragment size distribution:

$$f(M) = \text{const.}\exp\left[-\text{const.}\ M^{1/2}\right]\frac{d(M^{1/2})}{dM} \tag{A19a}$$

By Table 3, this is a Type II Weibull size distribution with

$$n/m = 1/2 \tag{A19b}$$

2.) Based on experimental data for "atomization of a liquid jet when a fast gas stream blows parallel to its surface," Marmottant & Villermaux (2004b) suggested a Type IIB Gamma size distribution with:

$$b = 2.81 \tag{A20}$$

Marmottant & Villermaux (2004b) relate the average fragment size D_{avg} to the average diameter D_0 of ligaments on the surface of the jet. More specifically, they say "the number of convolutions is, at most, such that the final average diameter D_{avg} restores D_0 or a fraction of D_0." In some cases, they normalize with D_0 rather than with D_{avg}.

3.) Based on experimental results for atomization of black liquor, Empie. al. (1993, 1995) suggested a Type IA root normal size distribution with:

$$\sigma = 0.20, \quad a = 1 \tag{A21}$$

Laney (2015a) showed that this is approximately equal to a Type IIB root normal size distribution with:

$$\sigma = 0.34,\ a = 0.9389 \tag{A22}$$

Figure A.5 shows four views of the Type II Weibull size distribution given by Equation (A19), the Type IIB Gamma size distribution given by Equation (A20), and the Type IIB root normal size distribution given by Equation (A22). These three size distributions are compared to each other and to experimental data for liquid atomization due to Turner & Moulton (1953) and experimental data for solid fragmentation due to Bewick et. al. (2015). Bewick et. al. (2015) used an explosively-driven 6.5-inch-diameter shock tube to load a 2-inch-thick precast concrete plate to a peak overpressure of approximately 4,000psi. In this case, the three size distributions agree with each other and with the experimental data to a rather remarkable degree.

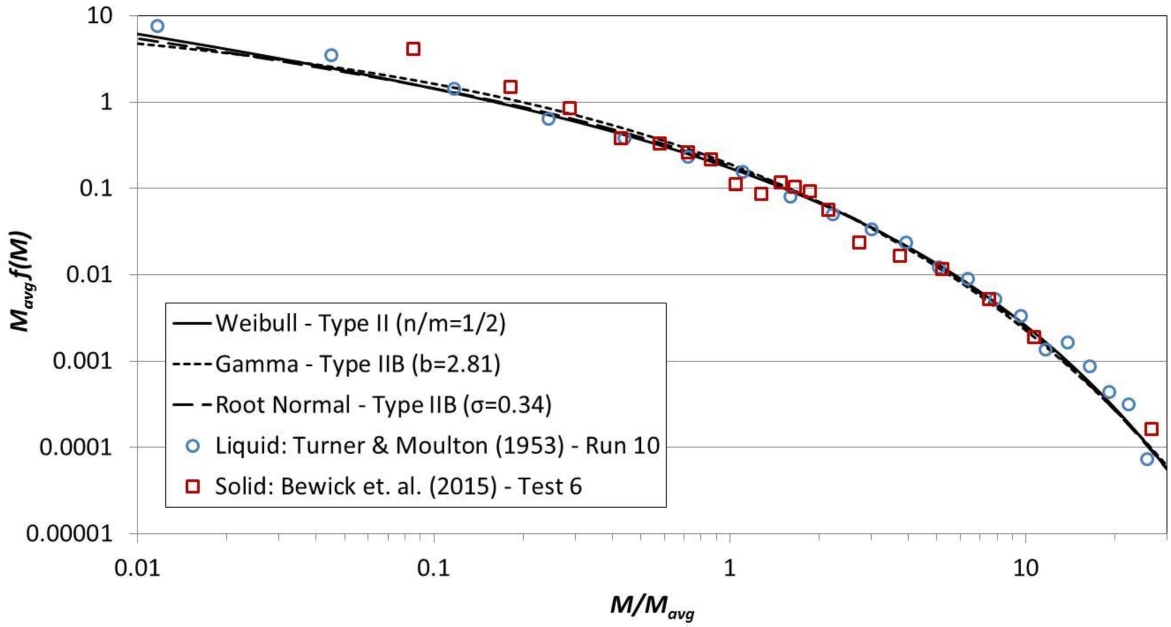

(a.) $f(M)$ in the log-log plane

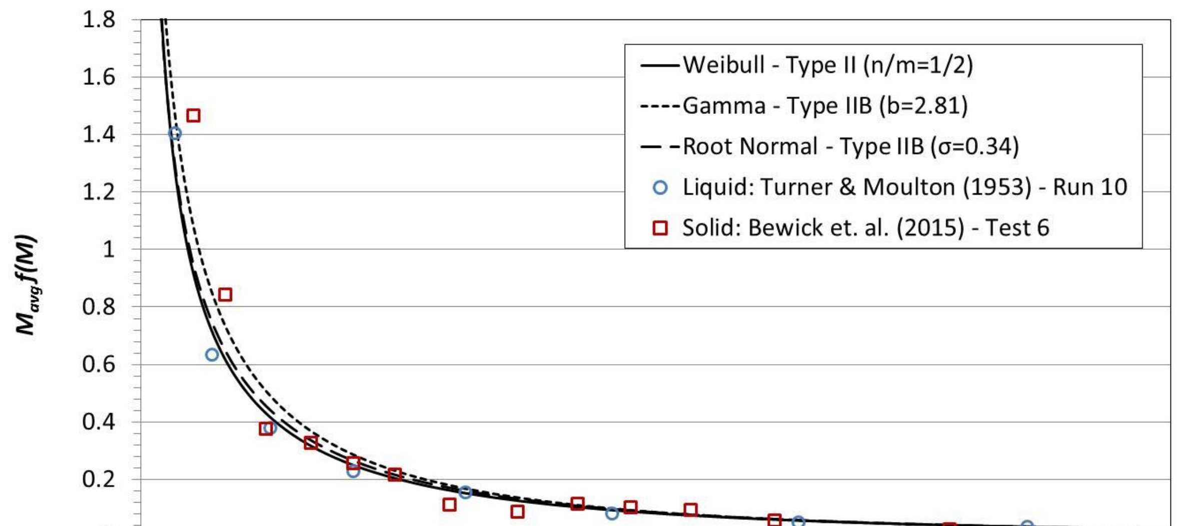

(b.) $f(M)$ in the linear-linear plane

Figure A.5. Type II Weibull, Gamma, and root normal size distributions vs. experimental data for liquid atomization due to Turner & Moulton (1953) and experimental data for solid fragmentation due to Bewick et. al. (2015). The Weibull, Gamma, and root normal size distributions all have R_M = 1.2±0.008.

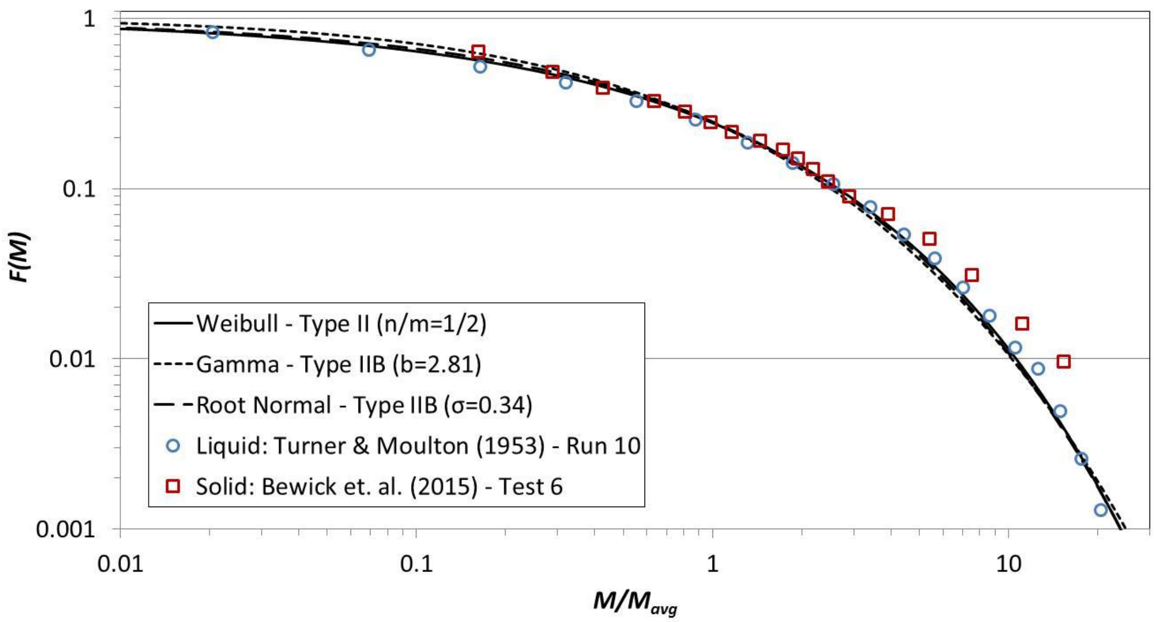

(c.) ***F*(*M*) in the log-log plane**

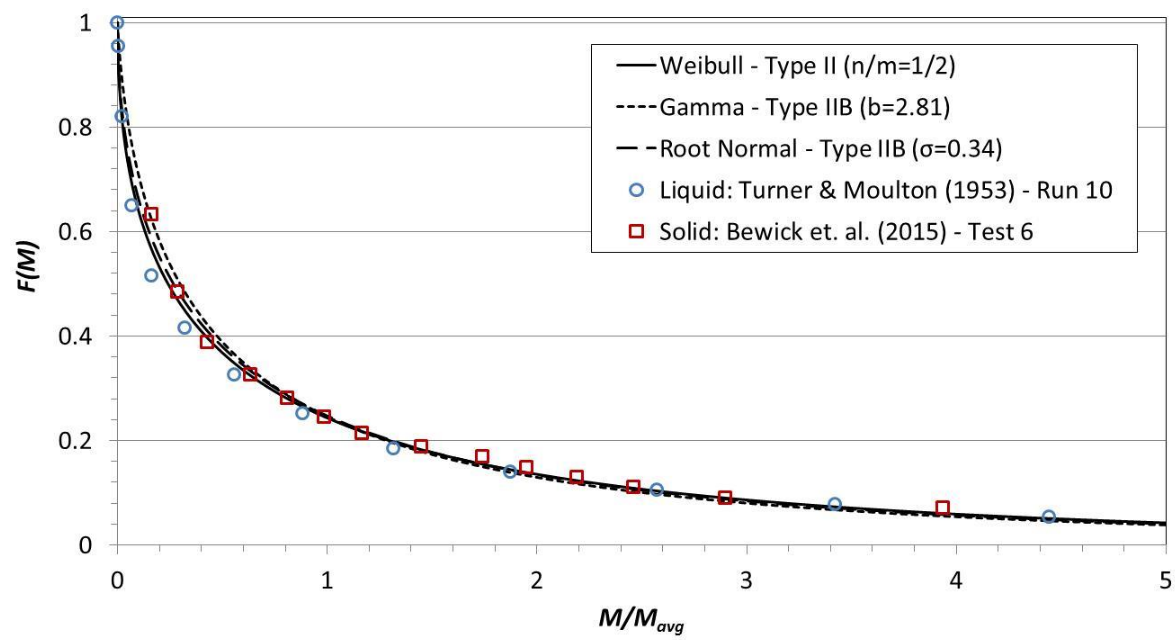

(d.) ***F*(*M*) in the linear-linear plane**

Figure A.5. ***(continued)***

A.6 Example 6

This example concerns fragment size distributions with $R_M = 1.25 \pm 0.012$. These distributions are considered to have a wide-to-very-wide size spread.

1.) For cylindrical high-explosives detonated inside cylindrical metal shells, Cohen (1981) suggested a Type II Weibull size distribution with:

$$n/m = 0.43 \tag{A23}$$

2.) Based on experimental results for acoustic breakup of thin liquid sheets, Mulmule et.al. (2010) suggested a Gamma size distribution with:

$$b = 2.2 \tag{A24}$$

3.) Based on over 2,000 liquid atomization experiments, Simmons (1977) suggested a Type IA root normal size distribution with $R_M = 1.2$ or equivalently:

$$\sigma \approx 0.238, \quad a = 1 \tag{A25}$$

Laney (2015a) showed that this is approximately equal to a Type IIB root normal size distribution with $R_M = 1.253$ or equivalently:

$$\sigma = 0.47, \ a = 0.8650 \tag{A26}$$

Figure A.6 shows four views of the Type II Weibull size distribution given by Equation (A23), Type II Gamma size distributions given by Equation (A24), and the Type IIB root normal size distribution given by Equation (A26). These three size distributions are compared to each other and to experimental data for liquid atomization due to Tate & Olson (1962) and experimental data for solid fragmentation due to Bewick et. al. (2015). Bewick et. al. (2015) used an explosively-driven 6.5-inch-diameter shock tube to load a 2-inch-thick precast concrete plate to a peak overpressure of approximately 1,500psi. In this case, the three size distributions agree well with each other and with the experimental data, except for the power law tail in the solid fragmentation data.

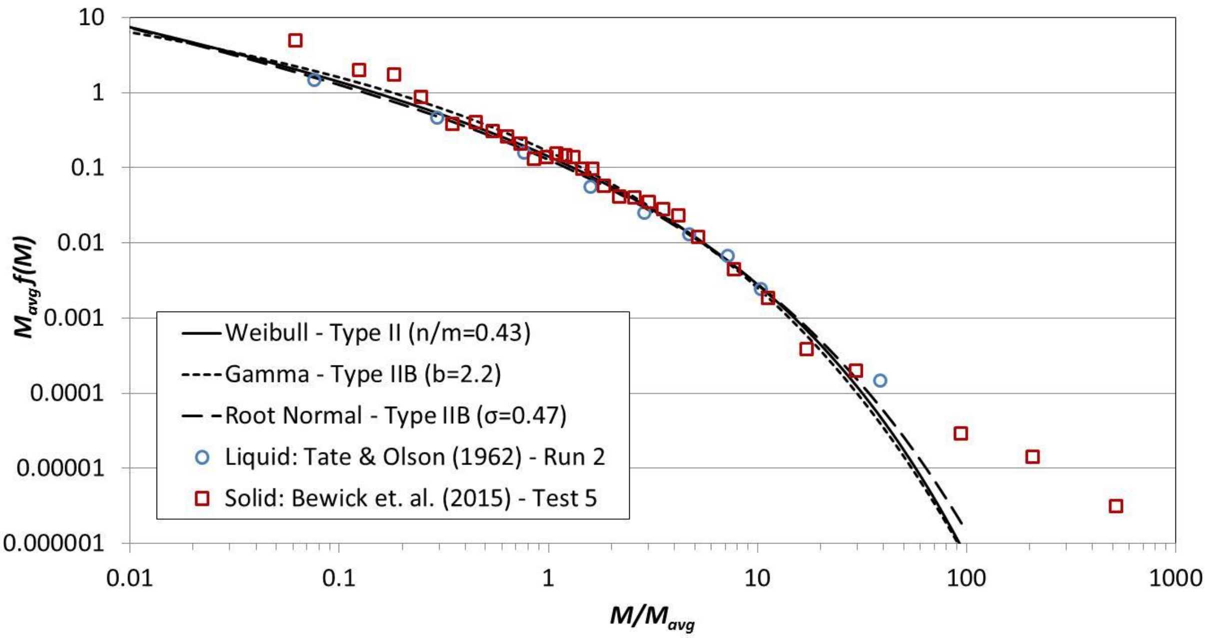

(a.) *f*(*M*) in the log-log plane

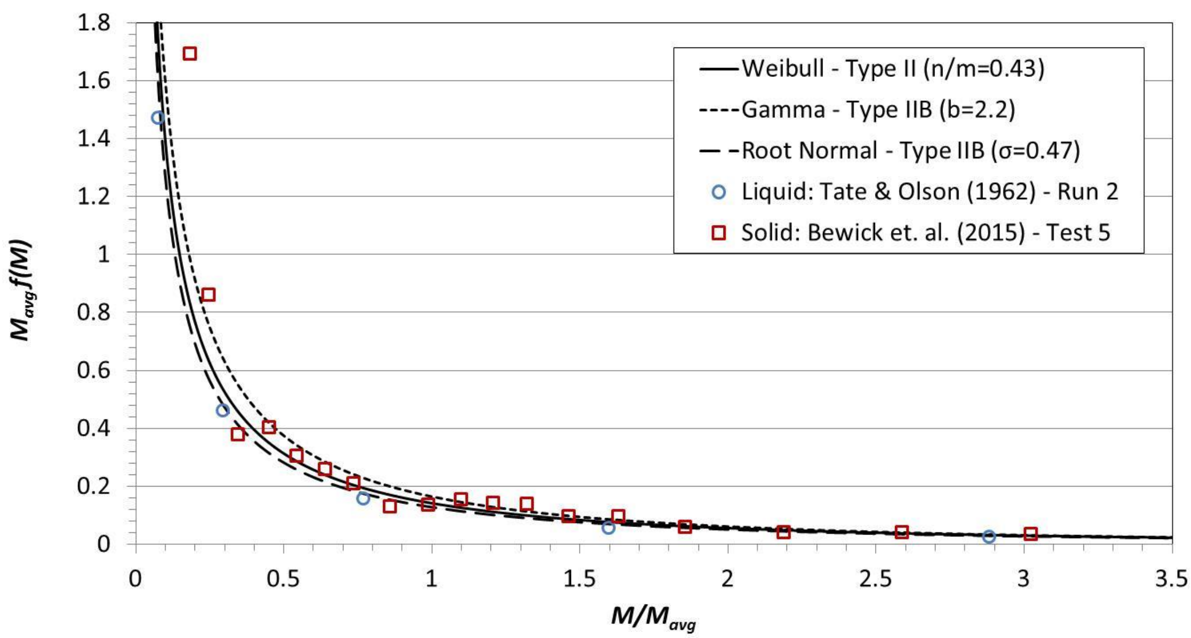

(b.) *f*(*M*) in the linear-linear plane

Figure A.6. Type II Weibull, Gamma, and root normal size distributions vs. experimental data for liquid atomization due to Tate & Olson (1962) and experimental data for solid fragmentation due to Bewick et. al. (2015). The Weibull, Gamma, and root normal size distributions all have R_M = 1.25±0.012.

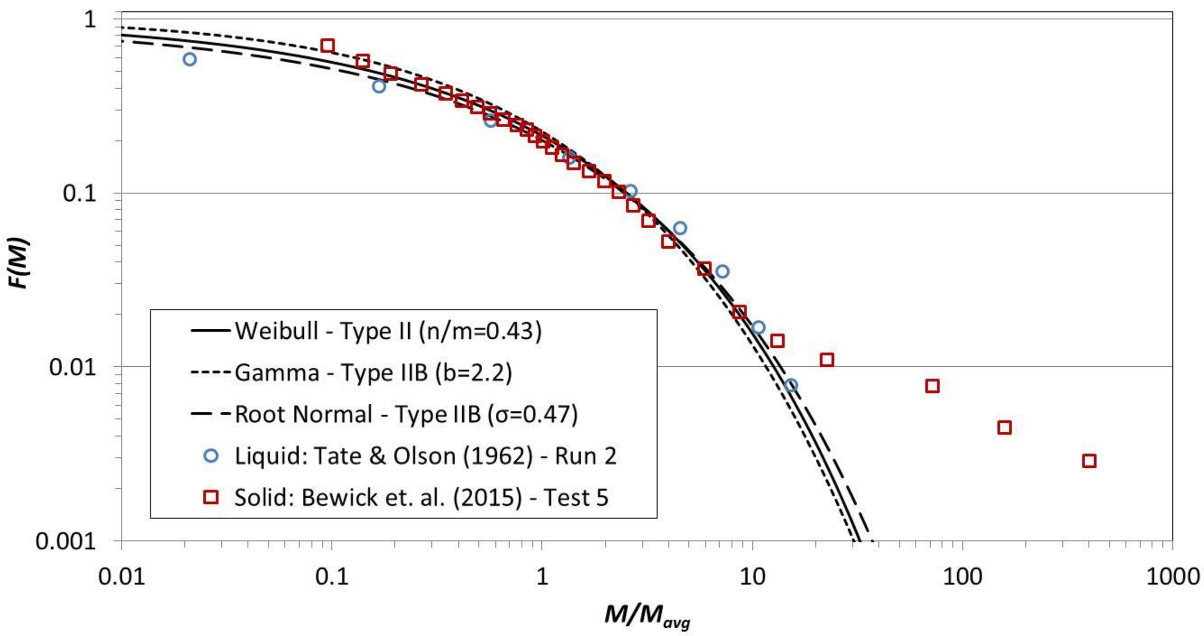

(c.) ***F*(*M*) in the log-log plane**

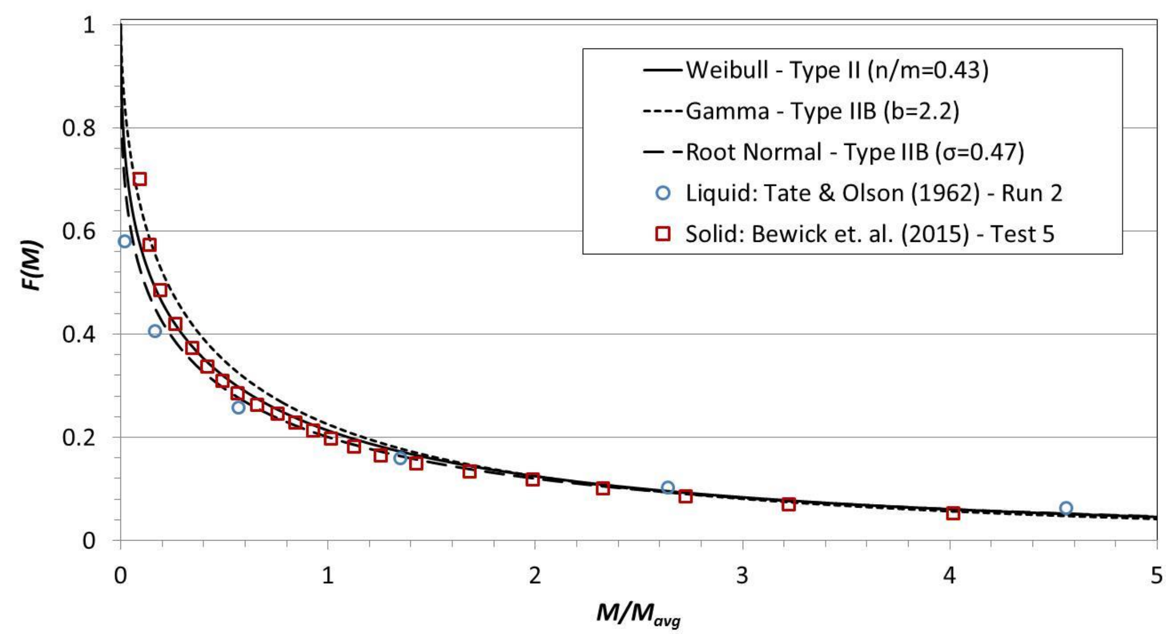

(d.) ***F*(*M*) in the linear-linear plane**

Figure A.6. ***(continued)***

A.7 Example 7

This example concerns fragment size distributions with $R_M = 1.333$ exactly. These distributions are considered to have a very wide size spread.

1.) Based on test results for cylindrical high-explosives detonated inside cylindrical metal shells, Mott & Linfoot (1943) suggested the following fragment size distribution:

$$f(M) = \text{const.}\exp\left[-\text{const.}\ M^{1/3}\right]\frac{d(M^{1/3})}{dM} \tag{A27a}$$

By Table 3, this is a Type II Weibull size distribution with

$$n/m = 1/3 \tag{A27b}$$

2.) Based on measurements of raindrops with *m* = 3, Marshall & Palmer (1948) suggested the following size distribution:

$$f(D) = \text{const.}\exp[-\Lambda D] \tag{A28a}$$

where the constant Λ depends on the rate of rainfall. By Table 3, this is a Type II Weibull size distribution with:

$$n/m = 1/3 \tag{A28b}$$

Marshall & Palmer (1948) argue that this "distribution … is the type that would obtain if growing droplets were in continual danger of disintegration, the likelihood of disintegration being proportional to the increment in diameter or in distance of fall." Building on this remark, Villermaux & Bossa (2009) argue that this size distribution can be "understood from the fragmentation products of non-interacting, isolated drops." Notice that since n/m is the same, Equations (A27) and (A28) are the same.

3.) Using maximum entropy theory with *m* = 3, Cousin et. al. (1996) derived a two-parameter family of size distributions. Based on experimental data for pressure-swirl atomizers, Cousin et. al. (1996) focused specifically on the following size distribution:

$$f_M(D) = \text{const.}\left(\frac{D}{D_{ref}}\right)^3 \exp\left[-\text{const.}\,D\right] \tag{A29a}$$

By Table 3, this is a Type II Weibull size distribution with:

$$n/m = 1/3 \tag{A29b}$$

As usual, it makes no difference that Table 3 uses D_{avg} while Equation (A29) uses D_{ref} .

Notice that, since n/m is the same, Equations (A27), (A28), and (A29) are the same. This relationship has not been previously observed.

4.) Based on experimental results for atomization of black liquor, Spielbauer et. al. (1989) suggested a Type IA root normal size distribution with:

$$\sigma = 0.286, \quad a = 1 \tag{A30}$$

Laney (2015a) showed that this is approximately equal to a Type IIB root normal size distribution with:

$$\sigma = 0.72, \ a = 0.5738 \tag{A31}$$

Figure A.7 shows four views of the Type II Weibull size distribution given by Equations (A27), (A28), and (A29) and the Type IIB root normal size distribution given by Equation (A31). These size distributions are compared to each other and to experimental data for liquid atomization due to Spielbauer et. al. (1989) and experimental data for solid fragmentation due to Mock & Holt (1981, 1983). Mock and Holt (1981, 1983) detonated a 2.75kg cylindrical charge of Composition B high-explosive inside a 4.5 x 8 inch cylindrical iron shell. In this case, the size distributions agree well with each other and with the experimental data.

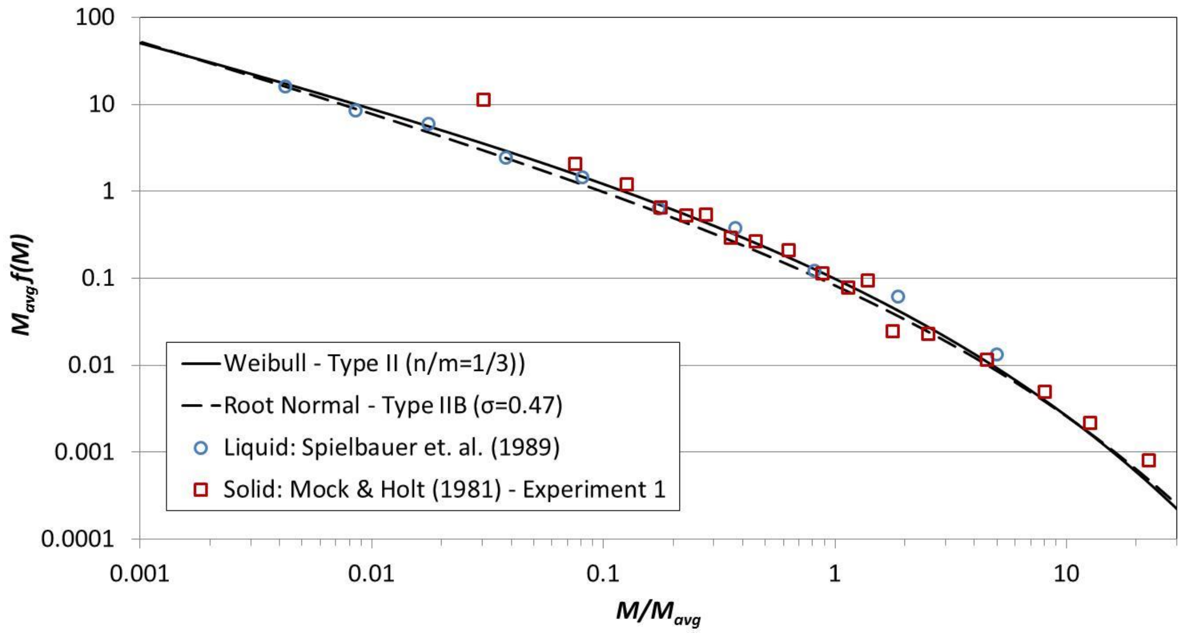

(a.) *f*(*M*) in the log-log plane

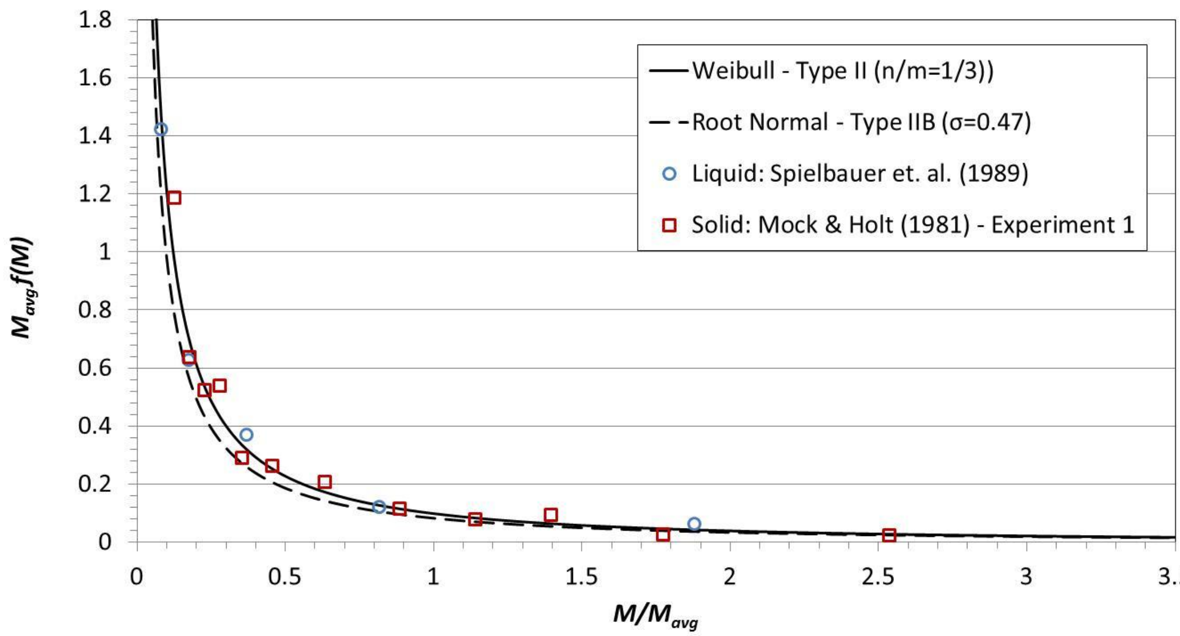

(b.) *f*(*M*) in the linear-linear plane

Figure A.7. Type II Weibull and root normal size distributions vs. experimental data for liquid atomization due to Spielbauer et. al. (1989) and experimental data for solid fragmentation due to Mock & Holt (1981). The Weibull and root normal size distributions have R_M = 1.333 exactly.

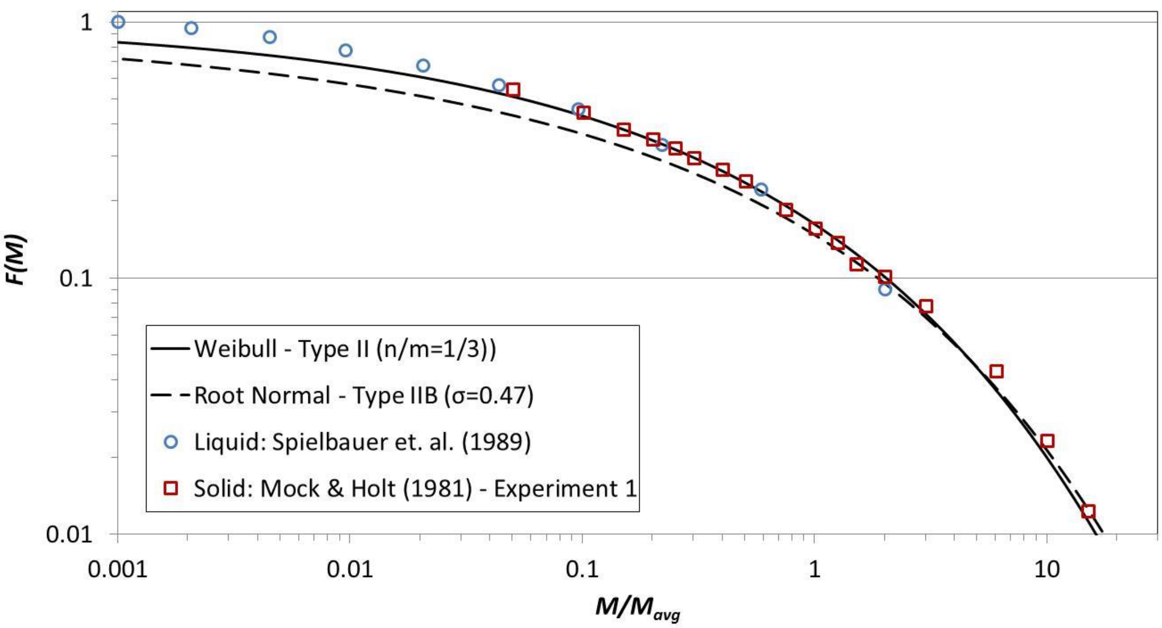

(c.) $F(M)$ in the log-log plane

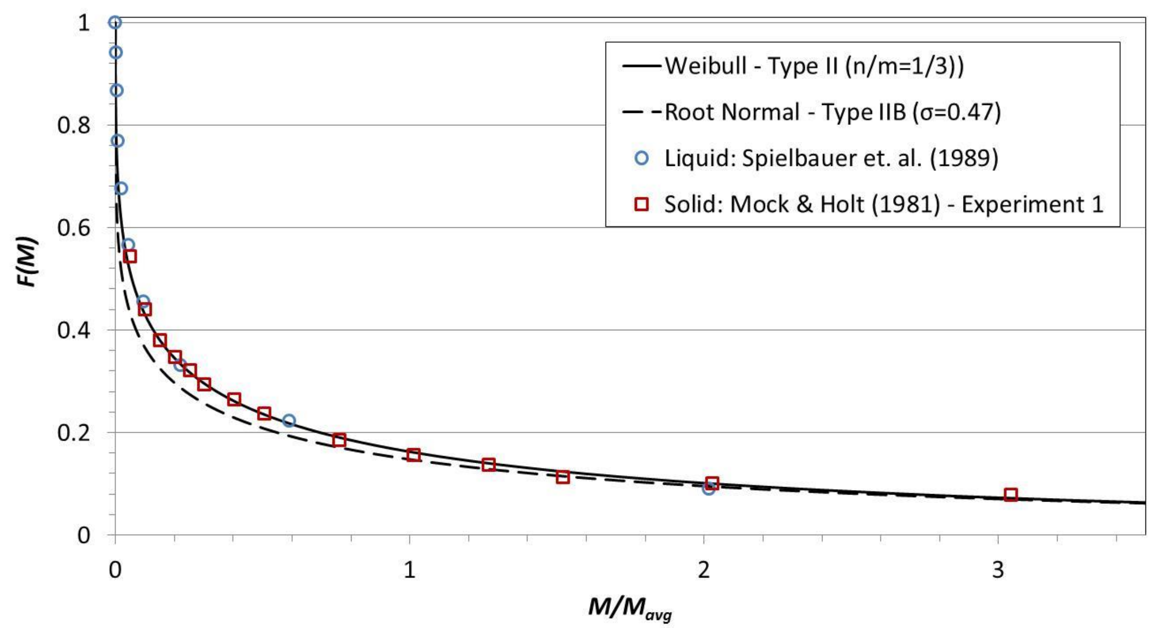

d.) $F(M)$ in the linear-linear plane

Figure A.7. ***(continued)***

References for Appendix A

M. M. Attarakih, H.-J Bart, and N. M. Faqir, Solution of the Droplet Breakage Equation for Interacting Liquid–Liquid Dispersions: A Conservative Discretization Approach, *Chemical Engineering Science*, 59, 2547 – 2565, 2004

B. Bewick, M. Barsotti, K. Marchand, M. Sanai, and A. Ziemba, Fragmentation Due To Overloaded Construction Facades, In M. G. Stewart and M. D. Netherton, Editors, *Design and Analysis of Protective Structures: Proceedings of the 3rd International Conference on Protective Structures*, Centre for Infrastructure Performance and Reliability, The University of Newcastle, 2015

N. Bremond and E. Villermaux, Atomization by Jet Impact, *Journal of Fluid Mechanics*, 549, 273-306, 2006

H. A. Carmona, F. K. Wittel, F. Kun, and H. J. Herrmann, Fragmentation Processes in Impact of Spheres, *Physical Review E*, 77, 051302, 2008

Y. S. Cheong, A. D. Salman, and M. J. Hounslow, Effect of Impact Angle and Velocity on the Fragment Size Distribution of Glass Spheres, *Powder Technology*, 138, 189-200, 2003

Y. S. Cheong, G. K. Reynolds, A. D. Salman, and M. J. Hounslow, Modelling Fragment Size Distribution using Two-Parameter Weibull Equation, *International Journal of Mineral Processing*, 74S, S227-S237, 2004

W.-H. Chou and G. M. Faeth, Temporal Properties of Secondary Drop Breakup in the Bag Breakup Regime, *International Journal of Multiphase Flow*, 24, 889-912, 1998

E. A. Cohen, New Formulas for Predicting the Size Distribution of Warhead Fragments, *Mathematical Modeling*, 2, 19-32, 1981

J. Cousin, S. J. Yoon, and C. Dumouchel, Coupling of Classical Linear Theory and Maximum Entropy Formalism for Prediction of Drop-Size Distribution in Sprays: Application to Pressure Swirl Atomizers, *Atomization and Sprays*, 6(5), 601-622, 1996

R. Cowan, New Classes of Random Tessellations Arising from Iterative Division of Cells, *Advances in Applied Probability*, 42(1), 26-47, 2010

H. J. Empie, S. J. Lien, R. S. Rumsey, and D. G. Sachs, *Kraft Black Liquor Delivery Systems Report No.4,* U.S. DOE Contract No. DE-FG02-88CE40839, IPST, Jan 1993

H. J. Empie, S. J. Lien, W. Yang, and T. N. Adams, Spraying Characteristics of Commercial Black Liquor Nozzles, *TAPPI Journal*, 78(1), 121-128, 1995

J.-S. Ferenc and Z. Néda, On the Size Distribution of Poisson Voronoi Cells, *Physica A*, 385(2), 518-526, 2007

D. E. Grady and M. E. Kipp, Geometric Statistics and Dynamic Fragmentation, *Journal of Applied Physics*, 58(3), 1985

D. E. Grady, L. T. Wilson, D. R. Reedal, L. D. Kuhns, M. E. Kipp, and J. W. Black, Comparing Alternate Approaches in the Scaling of Naturally Fragmenting Munitions, In I. R. Crewther, Editor, *Proceedings of the 19th International Symposium on Ballistics*, IBS, 2001

D. E. Grady and M. L. Olsen, A Statistics and Energy Based Theory of Dynamic Fragmentation, *International Journal of Impact Engineering*, 29, 293-306, 2003

T. Kiang, Random Fragmentation in Two and Three Dimensions, *Zeitschrift für Astrophysik*, 64, 433-439, 1966

C. B. Laney, *Improved Root Normal Size Distributions for Liquid Atomization*, Defense Threat Reduction Agency Technical Report DTRA-TR-16-003, November 2015

C. B. Laney, *Transformation and Self-Similarity Properties of Gamma and Weibull Fragment Size Distributions*, Defense Threat Reduction Agency Technical Report DTRA-TR-16-006, December 2015

K. E. J. Lehtinen and M. R. Zachariah, Self-Preserving Theory for the Volume Distribution of Particles Undergoing Brownian Coagulation, *Journal of Colloid and Interface Science*, 242, 314 –318, 2001

X. Li and R. S. Tankin, Droplet Size Distribution: A Derivation of a Nukiyama-Tanasawa Type Distribution Function, *Combustion Science and Technology*, 65–76, 1987

C. C. Lineau, Random Fracture of a Brittle Solid, *Journal of the Franklin Institute*, 221(4), 485-494, 1936

P. Marmottant and E. Villermaux, Fragmentation of Stretched Liquid Ligaments, *Physics of Fluids*, 16(8), 2732-2741, 2004a

P. Marmottant and E. Villermaux, On Spray Formation, *Journal of Fluid Mechanics*, 498, 73-111, 2004b

J. S. Marshall and W. McK. Palmer, The Distribution of Raindrops with Size, *Journal of Meteorology*, 5(4), 165–166, 1948

W. Mock and W. H. Holt, *Computational and Experimental Determination of Fragmentation for Naturally Fragmenting Warheads*, NSWC TR 80-238, May 1981

W. Mock and W. H. Holt, Fragmentation Behavior of Armco Iron and HF-1 Steel Explosive-Filled Cylinders, *Journal of Applied Physics*, 54(5), 2344-2351, 1983

N. F. Mott and E. H. Linfoot, *A Theory of Fragmentation*, U. K. Ministry of Supply, AC3348, January 1943

N. F. Mott, Fragmentation of Shell Cases, *Proceedings of the Royal Society A*, 189(1018), 300-308, 1947

G. W. Mulholland and H. R. Baum, Effect of Initial Size Distribution on Aerosol Coagulation, *Physical Review Letters*, 45, 761-763, 1980

A. S. Mulmule, M. S. Tirumkudulu, and K. Ramamurthi, Instability of a Moving Liquid Sheet in the Presence of Acoustic Forcing, *Physics of Fluids*, 22, 022101, 2010

R. Pimentel, R. Stowe, P. Harris, A. DeChamplain, and D. Kretschmer, Spray Characterization Based on the Pearson System of Frequency Curves, *Atomization and Sprays*, 20(5), 365-386, 2010

K.A. Sallam, C. Aalburg, G.M. Faeth, K.-C. Lin, C.D. Carter, and T.A. Jackson, Primary Breakup of Aerated-Liquid Jets in Supersonic Crossflows, *Atomization and Sprays*, 16(6), 657-672, 2006

T. M. Spielbauer, T. N. Adams, J. E. Monacelli, and R. T. Bailey, Droplet Size Distribution of Black Liquor Sprays, *Proceedings of the International Chemical Recovery Conference*, Ottawa, Canada, TAPPI/CPPA, 1989

G. M. Turner and R. W. Moulton, Drop Size Distributions from Spray Nozzles, *Chemical Engineering Progress*, 49(4), 185-190, 1953

E. Villermaux, Fragmentation, *Annual Review Fluid Mechanics*, 39, 419-446, 2007

E. Villermaux and B. Bossa, Single-Drop Fragmentation Determines Size Distribution of Raindrops, *Nature Physics*, 5, 697 – 702, 2009

F. K. Wittel, H. A. Carmona, F. Kun, and H. J. Herrmann, Mechanisms in Impact Fragmentation, *International Journal of Fracture*, 154(1-2), 105-117, 2008

F. Zhou, J.-F. Molinari, and K. T. Ramesh, Characteristic Fragment Size Distributions in Dynamic Fragmentation, *Applied Physics Letters*, 88, 261918, 2006

DEPARTMENT OF DEFENSE

DEFENSE THREAT REDUCTION
AGENCY
8725 JOHN J. KINGMAN ROAD
STOP 6201
FORT BELVOIR, VA 22060
ATTN: P. CLEMENT

DEFENSE TECHNICAL
INFORMATION CENTER
8725 JOHN J. KINGMAN ROAD,
SUITE 0944
FT. BELVOIR, VA 22060-6201
ATTN: DTIC/OCA

**DEPARTMENT OF DEFENSE
CONTRACTORS**

QUANTERION SOLUTIONS, INC.
1680 TEXAS STREET, SE
KIRTLAND AFB, NM 87117-5669
ATTN: DTRIAC